Chapter 8

Pipeline transportation of natural gas*

8.1. Physical and physico-chemical properties of natural gas

In the following we shall be concerned only with those physical and physicochemical properties that affect the transmission of gas in pipelines; even those properties will be discussed only in so far as they enter into the relevant hydraulic theories.

8.1.1. Equation of state, compressibility, density, gravity

It is the gas laws or, in a broader scope, the equations of state concerning natural gas that describe the interrelationships of pressure, specific volume and temperature, all of which may be subsumed under the notion '*pVT* behaviour' of the gas. Natural gas is not ideal, and the deviation of its behaviour from the ideal gas laws is seldom negligible and occasionally quite considerable. For the purposes of practical calculations, those equations describing the *pVT* behaviour of real gases are to be preferred that account for deviation from ideal-gas behaviour by a single correction factor, based on a consideration valid for any gas. Such a consideration is the *theorem of corresponding states*, expressed in terms of state parameters reduced to the critical state: this theorem states the existence of a function of the reduced state parameters, $f(p_r, V_r, T_r) = 0$, that is valid for any gas. The *pVT* behaviour of natural gas can be described in terms of an equation of state corrected by the compressibility factor z:

$$pV = z\frac{R}{M}T \qquad 8.1-1$$

where V is thespeci fic volume valid at pressure p and temperature T; R is the universal gas constant, whose rounded-off value is 8314 J/(kmole. K). Any given gas is characterized by its specific gas constant, or simply gas constant,

$$R' = \frac{R}{M}. \qquad 8.1-2$$

By the theorem of corresponding states, the compressibility factors z of two gases are equal if the reduced state parameters of the two gases are

* This Chapter has been written in co-operation with Ferenc Patch.

equal, that is, if the gases are in the same corresponding state. Reduced pressure is

$$p_r = p/p_c$$

and reduced temperature is

$$T_r = T/T_c.$$

In the case of gas mixtures, reduced parameters of state are to be replaced by the pseudo-reduced parameters p_{pr} and T_{pr} defined in terms of the pseudocritical pressure and temperature p_{pc} and T_{pc}, both depending on gas composition, as follows:

$$p_{pr} = p/p_{pc} \qquad 8.1-3$$

and

$$T_{pr} = T/T_{pc}. \qquad 8.1-4$$

If gas composition is known, p_{pc} and T_{pc} can be determined by applying the principle of additivity or—usually at a lower accuracy—using empirical diagrams. Additivity means that molar mass, pseudocritical pressure and pseudocritical temperature of a mixture can be added up from the respective parameters of the components, combined with their molar fractions or volume fractions:

$$M = \sum_{i=1}^{n} y_i M_i$$

$$p_{pc} = \sum_{i=1}^{n} y_i p_{ci}$$

$$T_{pc} = \sum_{i=1}^{n} y_i T_{ci}.$$

The accuracy of this calculation is usually impaired by the circumstance that, in the composition of the gas, the relative abundance of the heaviest components is given by a single figure denoted C_{n+}. The critical parameters are usually put equal to those of the component C_{n+1}; if e.g. the combined heavy fraction is C_{6+}, then it is taken into account with the critical parameters of heptane, C_7. This is, of course, an approximation whose accuracy depends on the actual composition of the combined heavy fraction.

Example 8.1—1. Find the molar mass and pseudocritical parameters of state at a pressure of 88 bars and 280 K temperature of the wet natural gas whose composition is given in Columns (1) and (2) of Table 8.1—1. The physical constants of the gas components are listed in Table 6.4—1. The calculation whose details are given in Columns (3), (4) and (5) of Table 8.1—1, furnishes $M = 21.5$ kg/kmole. By Eqs 8.1—3 and 8.1—4,

$$p_{pr} = \frac{8.8 \times 10^6}{4.59 \times 10^6} = 1.92$$

and

$$T_{pr} = \frac{280.0}{224.2} = 1.25.$$

Table 8.1—1

Components of natural gas	z_i	$M_i z_i$	$T_{ci} z_i$	$p_{ci} z_i$
		kg/kmol	K	10^5 N/m^2
1	2	3	4	5
Methane	0.790	12.67	150.7	36.67
Ethane	0.100	3.01	30.5	4.89
Propane	0.055	2.43	20.3	2.34
i-Butane	0.010	0.58	4.1	0.36
n-Butane	0.015	0.87	6.4	0.57
n-Pentane	0.024	1.73	11.3	0.81
CO_2	0.001	0.04	0.3	0.08
N_2	0.005	0.14	0.6	0.17
Total	1.000	21.47	224.2	45.90

Figure 8.1—1 permits us to read off pseudocritical pressures v. pressure and pseudocritical temperatures v. temperature for hydrocarbon gases of various molar mass.

Example 8.1—2. Find using Fig. 8.1—1 pseudoreduced parameters of state for a gas of molar mass $M = 21.5$ at the pressure and temperature stated in the foregoing example. — Figure 8.1—1 furnishes $p_{pc} = 4.61$ MN/m^2 and $T_{pc} = 223$ K. — By Eqs 8.1—3 and 8.1—4,

$$p_{pr} = \frac{8.8 \times 10^6}{4.61 \times 10^6} = 1.91$$

and

$$T_{pr} = \frac{280}{223} = 1.26.$$

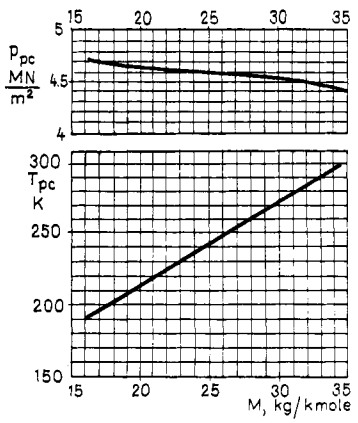

Fig. 8.1—1 Pseudocritical parameters of natural gas v. molar mass (from Katz 1959, p. 111; used with permission of McGraw-Hill Book Company)

The results furnished by the two procedures are in approximate agreement, but more substantial deviations may occur in other cases. Empirical diagrams other than Fig. 8.1—1 have been published (e.g. Stearns et al. 1951).

The compressibility factor z can be determined most accurately by laboratory experiments on pVT behaviour. If no $z = f(p, T)$ diagram based on experiment is available, then z is determined as a function of the reduced state parameters out of empirical diagrams or relationships. One of the best-known empirical diagrams is that of Standing and Katz (1942; Fig. 8.1—2). For the pseudoreduced parameters $p_{pr} = 1.92$ and $T_{pr} = 1.25$ of Example 8.1—1, it furnishes $z = 0.92$.

Natural gas often contains substantial amount of non-hydrocarbon gases, N_2 and CO_2 first of all. If the volume percentage of these is less than 8 percent for N_2 and 10 percent for CO_2, then the compressibility factor is

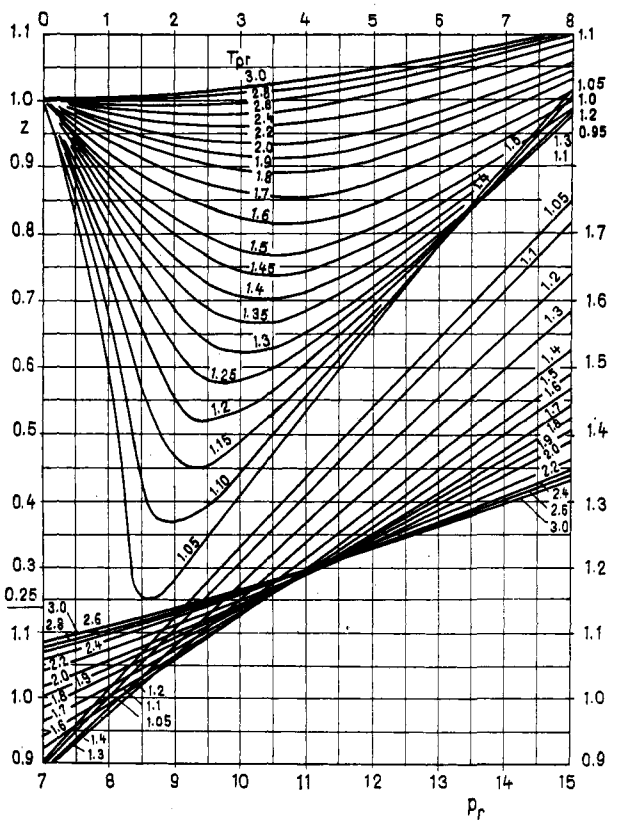

Fig. 8.1—2 Compressibility factor of natural gas v. pseudo-reduced parameters of state, after Standing (1952; reproduced by permission of the copyright owner—copyright © Chevron Research Company 1951; all rights reserved under the International Copyright Convention)

most readily determined by a procedure suggested by Gráf (Szilas 1967): the hydrocarbons are considered to be a single component whose pseudo-critical parameters and compressibility factors z are determined separately by some suitable method. The compressibility factors z_{CO_2} and z_{N_2} for CO_2 and N_2 are then read off Figures 8.1—3 and 8.1—4, and the value z' for the mixed gas as a whole is calculated using the mixing rule

$$z' = y_{N_2} z_{N_2} + y_{CO_2} z_{CO_2} + (1 - y_{N_2} - y_{CO_2}) z.$$

In writing computer programs it is an advantage if the compressibility factor can be found by calculation, without having to resort to diagrams. Literature contains several calculation procedures. The relevant formulae are mathematical representations of more or less extensive domains of the families of curves constituting the empirical diagrams. The French gas

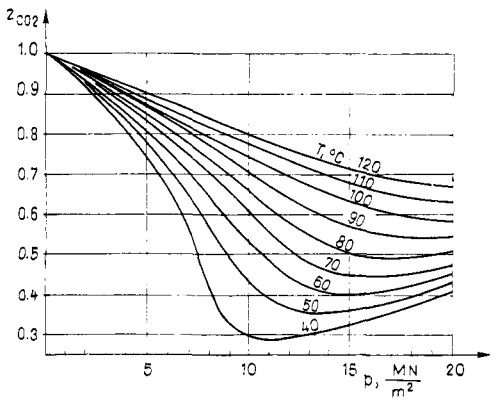

Fig. 8.1—3 Compressibility factor of CO_2 according to Reamer and Elters; after Török et al. (1966)

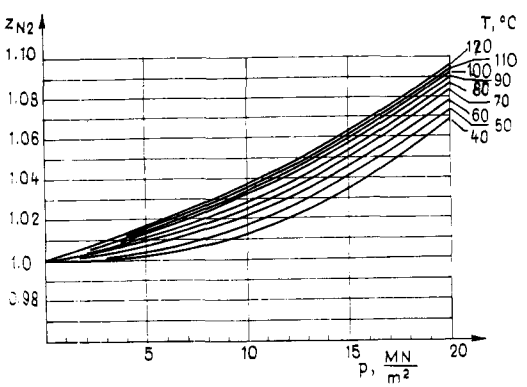

Fig. 8.1—4 Compressibility factor of N_2 according to Sage and Lacey; after Török et al. (1966)

industry uses for pressures of below 70 bars at soil-temperature flow the formula

$$z = 1 - 2 \times 10^{-8} p. \qquad 8.1-5$$

(Société . . . Manuel 1968). A relationship accounting also for temperature, applicable below 60 bars, is

$$z = \frac{1}{1 + kp} \qquad 8.1-6$$

k is listed for certain temperatures in Table 8.1—2 (likewise from Société . . . Manuel 1968).

Table 8.1—2

T °C	k
0	2.65×10^{-8}
15	2.04×10^{-8}
30	1.65×10^{-8}

Relationships for calculating the pseudocritical parameters of state have been given by Thomas et al. (1970)

$$p_{pc} = 4.894 \times 10^6 - 4.050 \times 10^5 \varrho_r \qquad 8.1-7$$

$$T_{pc} = 94.71 + 170.7 \varrho_r. \qquad 8.1-8$$

Wilkinson (1964) gave for $p_r < 1.5$ the formula

$$z = 1 + 0.257 p_{pr} - 0.533 \frac{p_{pr}}{T_{pr}} \qquad 8.1-9$$

where p_{pr} and T_{pr} are the values furnished by Eqs 8.1—3 and 8.1—4, respectively.

Gas density at pressure p and temperature T can be obtained putting $V = 1/\varrho$ in Eq. 8.1—1:

$$\varrho = \frac{pM}{zRT}. \qquad 8.1-10$$

If this equation is written up for the standard state, then $p = p_n$, $T = T_n$ and $z = z_n = 1$. Then

$$\varrho_n = \frac{p_n M}{R T_n}. \qquad 8.1-11$$

Let e.g. $p_n = 1.013$ bar and $T_n = 273.2$ K. Since furthermore, $R = 8314$ J/(kmole. K),

$$\varrho_n = \frac{M}{22.42}. \qquad 8.1-12$$

Rearranging we get, at the standard-state parameters stated above, the standard molar volume

$$V_{\text{mol}} = M\varrho_n = 22.42 \text{ m}^3/\text{kmole}. \qquad 8.1-13$$

Relative density is the standard-state density of the gas referred to the standard-state density of air:

$$\varrho_r = \frac{\varrho_n}{\varrho_{an}}. \qquad 8.1-14$$

Now by Eqs 8.1—12 and 8.1—14,

$$\varrho_r = \frac{M}{M_a} = \frac{M}{28.96}. \qquad 8.1-15$$

Gravity is

$$\gamma = \varrho g. \qquad 8.1-16$$

8.1.2. Viscosity

Gas viscosity, as distinct from liquid viscosity, increases as temperature increases, decreases as molecular weight increases, and is independent of pressure at medium pressures. At atmospheric pressure, viscosities of hydrocarbon gases vary linearly with temperature between 0 and 200 °C (Fig. 8.1—5). The viscosity of hydrocarbon mixtures at atmospheric pressures is readily calculated using a relationship published by Herning and Zipper:

$$\mu_a = \frac{\sum_{i=1}^{n} \mu_{ai} y_i \sqrt{M_i}}{\sum_{i=1}^{n} y_i \sqrt{M_i}}. \qquad 8.1-17$$

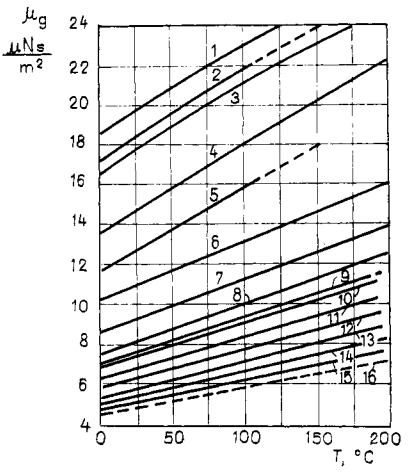

Fig. 8.1—5 Viscosities of natural gas components at atmospheric pressure; after Carr (1954). *1* helium, *2* air, *3* nitrogen, *4* carbon dioxide, *5* hydrogen sulphide, *6* methane, *7* ethane, *8* propane, *9* isobutane, *10* n-butane, *11* n-pentane, *12* n-hexane, *13* n-heptane, *14* n-octane, *15* n-nonane, *16* n-decane

Figure 8.1—6 is a plot of values furnished by this relationship, and, more generally, of measured viscosities of artificial hydrocarbon-gas mixtures. It permits us to find atmospheric pressure viscosity in terms of the molecular weight and relative gravity of the gas (Carr et al. 1954). The influence of non-hydrocarbon components may be taken into account by a viscosity-increasing correction depending on relative density, provided

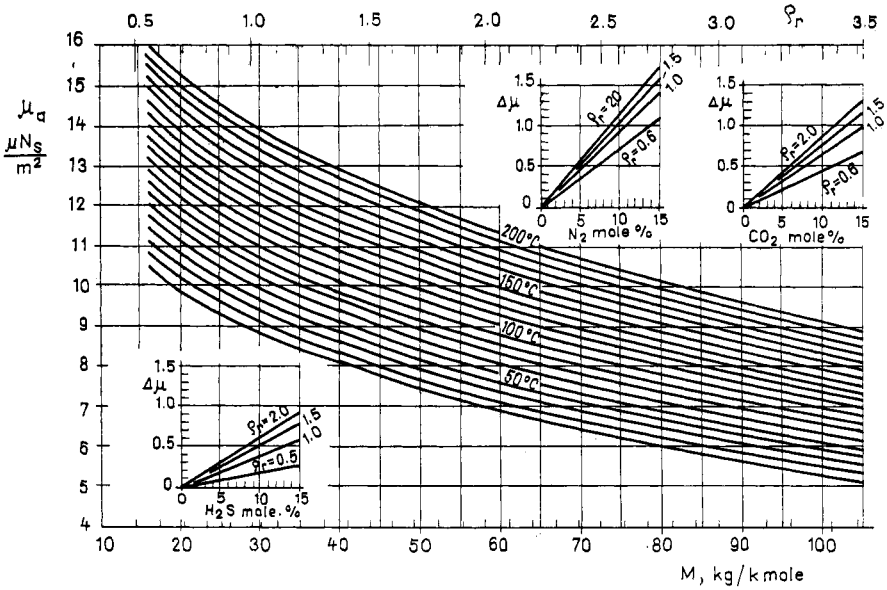

Fig. 8.1—6 Viscosity of natural gas at atmospheric pressure (Carr et al. 1954)

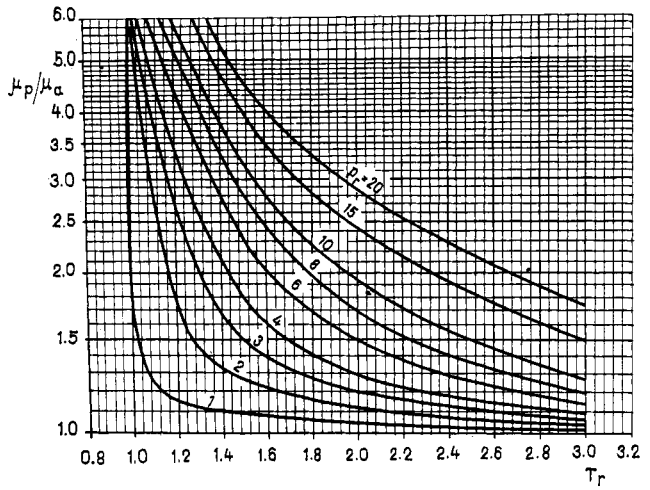

Fig. 8.1—7 Variation of $k = \mu_p/\mu_a$ v. the pseudo-reduced parameters of state (Carr et al. 1954)

the share of these components does not exceed 15 percent. — A relationship between viscosity and pressure may be set up making use of the theorem of corresponding states. Figure 8.1—7 allows us to find, in the knowledge of the pseudocritical pressure and temperature, the factor $k = \mu_p/\mu_a$ by which the viscosity at atmospheric pressure is to be multiplied in order to obtain the value that holds at pressure p (Carr et al. 1954). The relationship is valid in the gaseous state only, and it is therefore necessary in critical cases to check by phase examinations whether or not a liquid phase is present.

8.1.3. Specific heat, molar heat, adiabatic gas exponent, Joule—Thomson effect

Specific heat is the heat capacity of the unit mass or molar mass of a substance or, in the case we are discussing, the ratio of the heat dQ imparted to a unit mass of gas to the resulting temperature change dT, provided no phase change takes place during the temperature change. The usual cases investigated in a gas are temperature changes at constant pressure, on the one hand, and at constant volume, on the other, and accordingly, two distinct specific heats may be defined, the isobaric c_p

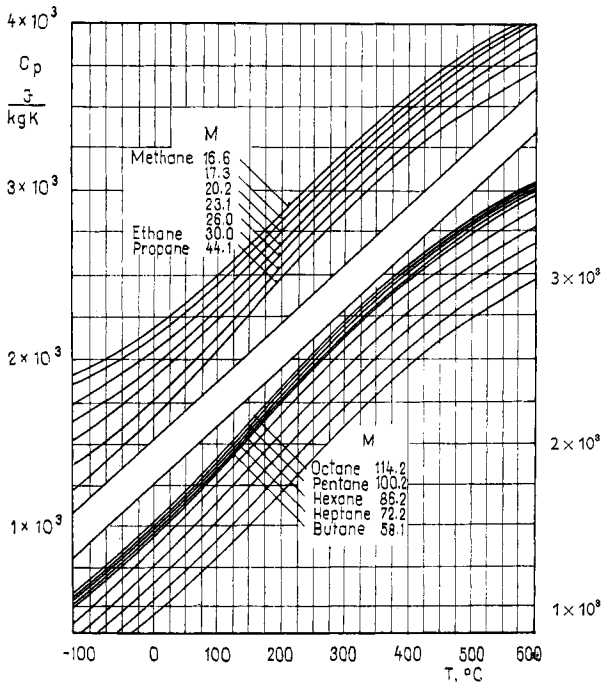

Fig. 8.1—8 Specific heats of natural-gas components at atmospheric pressure, after Brown (1945)

and the isochoric c_v. $c_p > c_v$, since part of the heat supplied to the system will expand the gas in the isobaric case. In ideal gases, the difference between the two constants equals the gas constant, that is,

$$c_p - c_v = R. \qquad 8.1-18$$

The difference between the characteristic specific heats in a real gas is not constant. Figure 8.1—8 after Brown (1945) shows isobaric molar heats v. temperature of hydrocarbon homologues at atmospheric pressure. The c_{pa} of gas mixtures can be determined on the basis of additivity, in terms of the components' specific heats and molar fractions, that is,

$$c_{pa} = \sum_{i=1}^{n} y_i \, c_{pai}.$$

The specific heat c_{pp} of a gas mixture at pressure p exceeds the value c_{pa} at atmospheric pressure by Δc_p. Figure 8.1—9 is a plot of Δc_p v. pseudo-

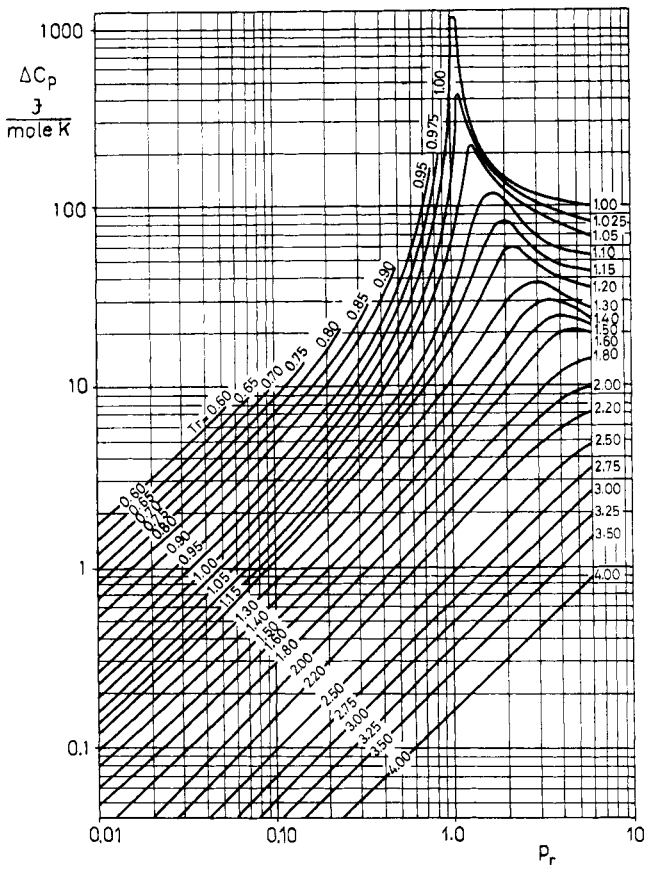

Fig. 8.1—9 Specific-heat correction, after Perry (1969)

reduced pressure p_{pr} for various pseudoreduced temperatures T_{pr} after Edmister (Perry 1969). Let us point out that Δc_p is stated in molar terms, and has to be divided by the molar M mass in order to transform it into a quantity having the nature of a specific heat.

The adiabatic gas exponent

$$\varkappa = \frac{c_p}{c_v} \qquad 8.1-19$$

is usually required in thermodynamic calculations. Its value can be determined, e.g., by reading the molar-heat difference $(c_p - c_v)$ off Fig.8.1—10

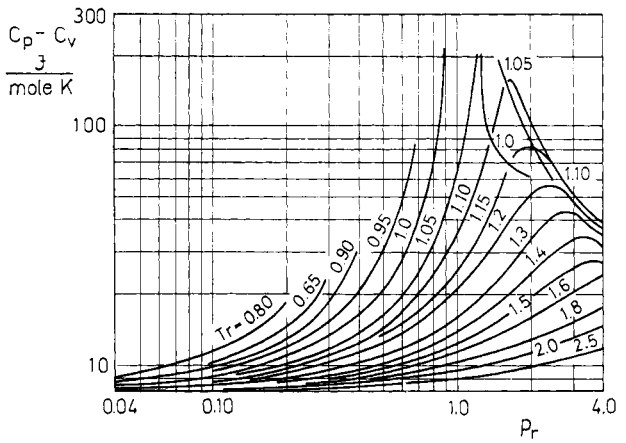

Fig. 8.1—10 $(c_p - c_v)$ of real gases v. the reduced parameters of state, after Perry (1969)

(after Perry 1969) and calculating c_v in the knowledge of c_p. The use of the figure presupposes knowledge of the pseudoreduced parameters of state. The molar heat or specific heat is calculated for a certain temperature range rather than for a single pair of pressure and temperature values. The mean molar heat c_p can be determined for instance by planimetering the specific heats calculated for various temperatures by the procedure outlined above. In a simpler procedure, one may read the enthalpy values h_1 and h_2 corresponding to the initial and terminal temperatures T_1 and T_2 off suitable diagrams or tables. Then

$$\bar{c}_p = \frac{h_2 - h_1}{T_2 - T_1}. \qquad 8.1-20$$

If the pressure of an ideal gas is lowered without the gas delivering energy, then, if the gas is ideal and the change of state is adiabatic, the total internal energy of the system remains unchanged, that is, the state change is isoenthalpic, and the temperature of the gas remains unchanged, too. If, however, the gas undergoing said change is real, then its volume change will differ from ideal gas behaviour. As a result, its internal energy

and hence also its temperature will be affected (Joule–Thomson effect). Among the temperature changes taking place during gas flow, it is expedient to account for this effect by the Joule–Thomson coefficient μ_d, which is a measure of temperature change per unity pressure change. $\mu_d \gtrless 0$, that is, expansion may increase, reduce or leave unchanged the

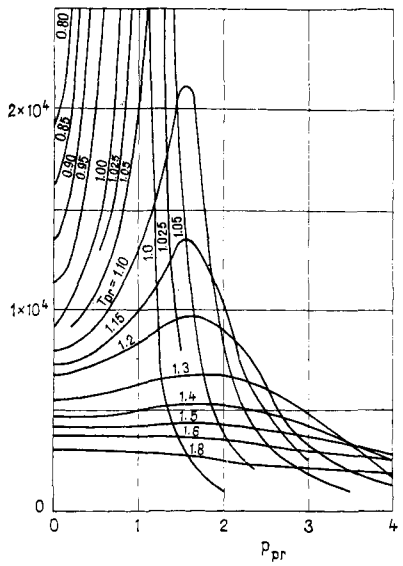

Fig. 8.1–11 Relationship for determining the choke effect, after Korchazhkin (1963)

temperature of the gas. Several relationships for determining μ_d have been derived. Figure 8.1–11 gives the values [in J/(K kmole)] of the expression

$$\frac{p_{pc}\, c_p\, \mu_d}{T_{pc}}$$

in terms of the pseudoreduced parameters of state, and this expression may be solved to yield μ_d (Korchazhkin 1963).

8.1.4. Hydrocarbon hydrates

Hydrocarbon gas hydrate is a solid granular substance resembling snow or ice. It is composed of water and the molecules of one or more hydrate-forming gases. The molecules of this gas enter cavities in the H_2O lattice, which is looser than the ice lattice, without entering into chemical bond with the water. The lattice thus forming may be one of two pentagonal dodecahedra. The conditions of hydrate formation and stability are: (i) sufficiently low temperature and high pressure; (ii) the hydrate-forming gas is held together by covalent bonds; its molecules are shorter than 8 Å;

and when liquid, it is immiscible with water; (iii) during hydrate formation, water is liquid; (iv) hydrate is resistant to water and no Van der Waals forces arise between its molecules.

Hydrates include besides water methane, ethane, propane or butane, alone or mixed together. In addition to the hydrocarbons, other, non-hydrocarbon gas components such as nitrogen, carbon dioxide or hydrogen sulphide may also be hydrate-forming. Hydrate composition depends on the nature of the hydrate-forming gas but is not governed by the rules of

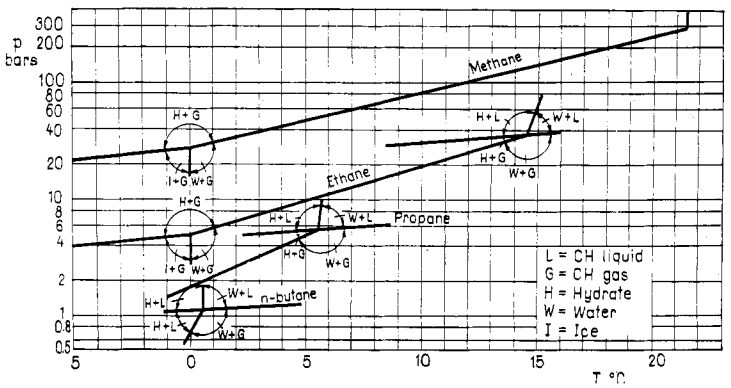

Fig. 8.1—12 State diagram of hydrocarbons according to Willard; after Orlicek and Pöll 1951, Table 118 (used with permission of Springer-Verlag, Wien/New York)

stoichiometry. The least water-to-methane ratio in methane hydrate would be 4.5, in view of the number of methane molecules that can be accommodated in the water lattice. However, methane-unsaturated hydrates with more than 4.5 moles of H_2O per mole of methane also occur. The least water content of ethane hydrate is about 7.7 moles H_2O per mole of ethane. The propane and butane molecules may enter but the largest cavities of the lattice, and hence, in propane hydrate, 17 moles at least of water are required per mole of propane.

Figure 8.1—12 shows state diagrams of various two-component hydrocarbon hydrates after Willard (Orlicek and Pöll 1951). The upper temperature limit e.g. of propane hydrate formation is seen to be 5.6 °C, with a corresponding pressure of 5.6 bars. The point defined by these parameters of state is an invariant of the propane-water system, a four-phase point with no degree of freedom, where propane hydrate as the solid phase is at equilibrium with gaseous propane saturated with water vapour, water saturated with liquid propane and propane saturated with water. The figure shows which phases may coexist in the individual regions. In reality, it is usual for hydrates to involve more than one hydrocarbon component. The critical pressure of hydrate formation is substantially reduced e.g. if methane is accompanied by some hydrocarbon of larger molar mass, propane or butane first of all. Even quite low concentrations of these may displace the phase diagram rather considerably. For approximate estimates

one may use Fig. 8.1—13, which shows critical hydrate-formation pressures and temperatures for hydrocarbons of various relative gravities. The presence of CO_2 and H_2S at a given temperature may lower the critical pressure, whereas the presence of N_2 tends to raise it. The inset in Fig. 8.1—13 provides the correction factor C_{N_2} which shows how many times the critical pressure of hydrate formation is higher in the presence than in the absence of a certain quantity of nitrogen.

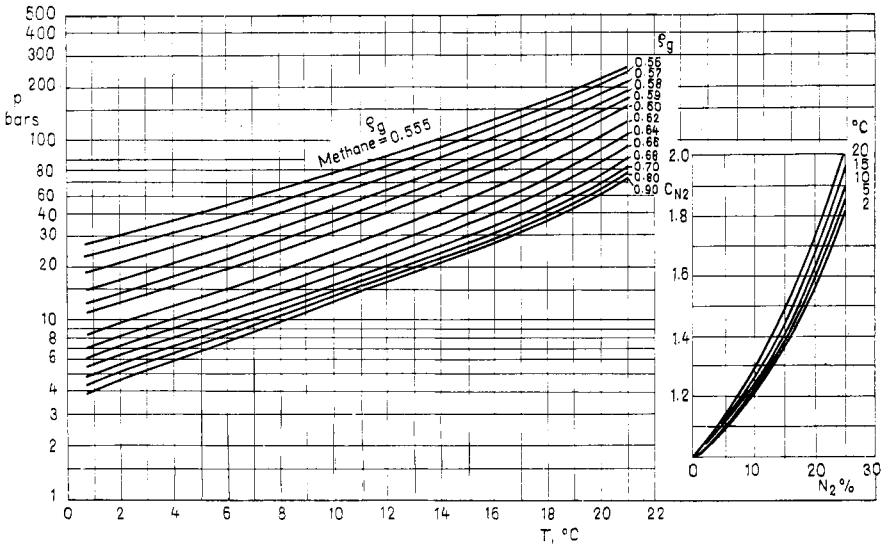

Fig. 8.1—13 Limits of gas hydrate formation, after Katz (1959, p. 213; used with permission of McGraw-Hill Book Company)

Several more accurate procedures have been devised. For nitrogenless natural gas, up to about 280 bars pressure, Katz' procedure involving equilibrium constants is best suited. The condition of hydrate formation is

$$\sum_{i=1}^{n} \frac{z_{hi}}{K_{hi}} = 1.$$

The K_{hi}s are to be read off the $K_h = f(T)_p$ diagrams of the hydrate-forming components (Katz 1959). — Heinze (1971) prefers the modified McLeod—Campbell procedure for determining hydrate formation temperatures (hydrate points) of natural gas containing nitrogen up to about 400 bars pressure. The hydrate point is calculated using the relationship

$$T = \sqrt{\frac{K_h}{0.445}}. \qquad 8.1-21$$

The values of K_h for various pressures are contained in Table 8.1—3. The K_h values falling between those given in the table may be found by

Table 8.1—3
Hydrate-equilibrium factors K_h for hydrate-forming natural-gas components (modified after Heinze 1971)

Components \ p, bars	50	100	150	200	250	300	350	390
CH_4	34,543	35,949	36,719	37,357	37,814	38,204	38,531	38,767
C_2H_6	45,535	47,101	48,078	48,704	49,316	49,772	50,140	50,435
C_3H_8	85,060	83,970	79,836	75,610	73,150	71,340	70,103	69,154
i-C_4H_{10}	102,096	94,310	89,319	82,481	78,791	75,569	74,533	73,304
n-C_4H_{10}	57,979	51,133	47,648	45,032	43,846	43,328	43,276	43,234
N_2	30,555	32,133	33,369	33,695	34,214	34,656	35,005	35,251
CO_2	38,788	43,504	44,812	46,773	50,371	51,660	52,269	54,018
H_2S	63,986	69,972	74,001	76,349	78,554	80,426	81,373	82,148

linear interpolation. The hydrate factor for multi-component natural gas of known molar ratios may be found by applying the principle of additivity.

Example 8.1—3 (Heinze 1971). Find the hydrate point at 147 bars pressure for the gas composition given in Column 2 of Table 8.1—4. Let us point out that, regardless of the quantity and nature of the longer-molecule non-hydrate-forming natural-gas components, it is assumed that

$$\sum_{i=1}^{n} z_{hi} = 1.$$

By the data in Column 4 of the Table, $K_h = 39{,}459$ and hence, hydrate point is at

$$T = \sqrt{\frac{39{,}459}{0.445}} = 297.8 \text{ K} = 24.6 \text{ °C}.$$

Hydrate point may be substantially reduced by adding to the natural gas a hydrate inhibitor such as calcium chloride, methanol, ethylene glycol, diethylene glycol.

Table 8.1—4
Finding the hydrate formation temperature of Thönse gas (after Heinze 1971)

Components	z_{hi}	K_{hi} at 147 bars	$z_{hi}K_{hi}$
CH_4	0.865	30,673	31,722
C_2H_6	0.073	48,020	3,505
C_3H_8	0.028	80,084	2,242
i-C_4H_{10}	0.013	89,618	1,165
N_2	0.010	33,295	333
CO_2	0.011	44,734	492

$\sum_{i=1}^{n} z_{hi}K_{hi} = 39{,}459$

8.2. Temperature of flowing gases

In most long uninsulated pipelines, the temperature of flowing gas approaches soil temperature after a travel sufficiently short for flow temperature to be identified for all practical purposes with soil temperature over the full length of the pipeline. In certain cases, however, the flow temperature of gas may significantly differ from the temperature of the surrounding soil, and it may then be important to determine temperature traverses for the pipeline. The cases in question include the following. (i) It is necessary to decide in designing where the flow temperature drops

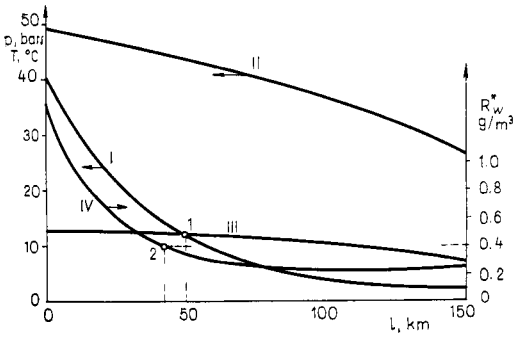

Fig. 8.2—1 Pinpointing hazard of hydrate formation in a pipeline, after Smirnov and Shirkovsky (1957) and Török et al. (1968)

below the hydrate point; (ii) it is desired to chill the gas by injecting liquefied gas, in order to increase the throughput capacity of the pipeline (Gudkov et al. 1970); (iii) in arctic regions, the gas may cause an undesirable warming up of the permafrost soil in which the pipeline is laid.

Figure 8.2—1 (after Smirnov and Shirkovsky 1957; and Török et al. 1968) is a temperature traverse of a given pipeline (Graph I). It permits us to delimit the line segment where there is a risk of hydrate formation. Graph II is the pressure traverse. The accurate calculation of the two traverses takes a successive-approximation procedure. In the knowledge of pressure, the hydrate-point traverse (Graph III) may be calculated in the manner explained in Section 8.1.4. At point *1*, where Graphs II and III meet ($l = 50$ km), the hydrate point T_h is just equal to the temperature T_g of gas flow. For hydrate to form, it is sufficient that there be some free water available at this line section. Graph IV is a water vapour saturation traverse along the pipeline. Points of this curve can be determined by means of auxiliary diagrams for corresponding pairs of p and T_g (e.g., Katz 1959). Assuming the water vapour content of the gas to be 0.4 g/m³, the dew point of the gas turns out to occur at point *2*; from there on, the pipeline does contain condensed water: that is, this condition of hydrate formation is also satisfied at and beyond $l = 50$ km.

The temperature of gas flowing in the pipeline depends, for a given inflow temperature T_1 and soil temperature T_s, on the following factors: (i) heat exchange with the environment, depending primarily on the heat

transfer coefficient (cf. Section 7.2.3). The internal convection coefficient, α_1, is infinite in a fair approximation. (ii) The Joule–Thomson effect due to friction, velocity increase and altitude change. (iii) Phase changes (condensation, evaporation) due to pressure and temperature changes. (iv) The energy loss of flow, which end up as heat.

These effects are accounted for in steady-state flow by the following equation (Pápay 1970), stating flow temperature at a distance l_x from the head end of the line to be

$$T_{lx} = \frac{C_1^{\frac{C_2}{C_3}} \left[T_s + \frac{C_4}{C_2} - \frac{C_1 C_5}{C_2(C_2 + C_3)}\right]}{(C_1 + C_2 l_x)^{\frac{C_2}{C_3}}} - \frac{C_4 + C_5 l_x}{C_2} + \frac{C_5(C_1 + C_3 l_x)}{C_2(C_2 + C_3)} \qquad 8.2-1$$

where

$$C_1 = z_{V1}\, c_{pL} + (1 - z_{V1})\, c_{pV}; \qquad C_2 = \frac{k}{q_m};$$

$$C_3 = \frac{z_{V2} - z_{V1}}{l}\, (c_{pL} - c_{pV})$$

$$C_4 = z_{V1}\, c_{pL}\, \mu_{dL} \frac{p_1 - p_2}{l} + (1 - z_{V1}) c_{pV}\, \mu_{dV} \frac{p_1 - p_2}{l} +$$

$$+ Q\, \frac{z_{V2} - z_{V1}}{l} + v_1 \frac{v_2 - v_1}{l} + g\, \frac{h}{l} - \frac{k\pi\, d_o}{q_m} T_1$$

$$C_5 = \frac{(z_{V2} - z_{V1})\,(p_1 - p_2)}{l^2}\, (c_{pL}\, \mu_{dL} - c_{pV}\, \mu_{dV}) + \left(\frac{v_2 - v_1}{l}\right).$$

In deriving this equation, Pápay assumed pressure, flow rate and phase transitions to be linear functions of distance from the head end. It is therefore recommended in problems where a high accuracy is required to calculate temperature changes for shorter line segments. Let us point out that suffix 1 invariably refers to the head end and 2 to the tail end of the line of length l, except, of course, in the numbering of the constants C.

In the case when the phase changes are left out of consideration—that is, in single-phase flow—Eq. 8.2–1 simplifies to

$$T_{lx} = T_s + (T_1 - T_s)\, e^{-al_x} - \frac{\mu_{dV}(p_1 - p_2)}{al} \times$$

$$\times\, (1 - e^{-al_x}) - \frac{gh}{al\, c_{pV}} (1 - e^{-al_x}) - \frac{v_2 - v_1}{al\, c_{pV}} \times$$

$$\times \left[\left(v_1 - \frac{v_2 - v_1}{al}\right)(1 - e^{-al_x}) + \frac{(v_2 - v_1)\, l_x}{l}\right] \qquad 8.2-2$$

where

$$a = \frac{k}{q_m\, c_{pV}}.$$

The first two terms of this equation describe heat exchange with the environment; the third one accounts for the Joule–Thomson effect, the fourth for the change in geodetic head and the fifth for the change in velocity head. In practical calculations, the last two terms may be neglected. The resulting error is usually less than the error due to uncertainties in the various parameters. If the pressure drop is small, then so is the temperature drop due to expansion, and the third term may also be neglected, in which case Eq. 8.2–2 simplifies to Eq. 7.2–15.

8.3. Steady-state flow in pipeline systems

The fundamental relationships of gas flow in a pipeline are stated in Section 1.2. That section refers to a single pipeline. Actual gas transmission systems, however, often form connected nets, in which flow is governed by relationships much more involved than those referring to a single line. Pipe nets may be high-pressure, with pressure changes entailing significant changes in specific volume, and low-pressure, with such changes negligible. The first type includes transmission systems of regional supply, the second includes gas nets supplying local consumer groups, most often community utilities and households. In the latter we shall concentrate on the first type.

Flow in transmission systems is almost invariably transient, but numerous design and operation control problems may be solved notwithstanding by assuming flow to be steady-state. Network models based on the assumption of steady flow permit the establishment of pressure contour maps of both radial and looped networks for periods of peak demand. This map permits us to pinpoint the critical segments of the net, where consumer demand cannot be fully met in peak demand periods. The pressure map is useful in designing new systems, and in expanding or checking the operation of existing ones.

8.3.1. Design fundamentals

The two basic elements of a pipeline network are the *nodes* and the *node connecting elements* (NCEs). Nodes include those points where a pipeleg ends, or where two or more NCEs join, or where there is injection or delivery of gas. The pressure map of the network is determined by node pressures. The most important NCEs are pipelegs, compressor stations, regulators, valves, and underground gas storages. Prior to constructing a model of a a complex system it is necessary to establish mathematical models for individual NCEs. These models are in effect pressure v. throughput relationships valid at given parameters.

The characteristic equation of a *high-pressure pipeleg* is, by Eq. 1.2–7,

$$p_1^2 - p_2^2 = k_1 q^2. \qquad 8.3-1$$

The gas flow expressed in standard volume units is

$$q = \left[\frac{p_1^2 - p_2^2}{k_1}\right]^{0.5} \qquad 8.3-2$$

where

$$k_1 = 1.95 \times 10^{-4} \left(\frac{p_n}{T_n}\right)^2 \frac{lM\,\bar{T}\bar{z}\,\bar{\lambda}}{d_i^5}. \qquad 8.3-3$$

In a *low-pressure pipeleg*, with pressure close to atmospheric, we have $\bar{z} = 1$ and

$$p_1^2 - p_2^2 = (p_1 + p_2)(p_1 - p_2) \approx 2p_n(p_1 - p_2)$$

and the above equations modify to

$$p_1 - p_2 = k_2 q^2 \qquad 8.3-4$$

and

$$q = \left[\frac{p_1 - p_2}{k_2}\right]^{0.5} \qquad 8.3-5$$

respectively, with

$$k_2 = 0.975 \times 10^{-4} \frac{p_n l M \bar{T} \bar{\lambda}}{T_n^2 d_i^5}. \qquad 8.3-6$$

Compressor characteristics are provided by the manufacturer. These may usually be approximated by a function of the type

$$q = \frac{P}{k_3 \left(\frac{p_2}{p_1}\right)^{k_4} + k_5} \qquad 8.3-7$$

where k_3, k_4 and k_5 are compressor constants.

Pressure regulators may be described by the flow equations of chokes (cf. Section 1.5—1). If the pressure drop is less than critical (flow is subsonic), then Eq. 1.5—2 will hold if the gas is liquidless, that is,

$$q = k_6 p_1 \sqrt{\left(\frac{p_2}{p_1}\right)^{\frac{2}{\varkappa}} - \left(\frac{p_2}{p_1}\right)^{\frac{\varkappa+1}{\varkappa}}} \qquad 8.3-8$$

where

$$k_6 = \sqrt{2R}\,\frac{\pi}{4}\,d_{ch}^2\,\frac{T_n}{p_n}\,\alpha \sqrt{\frac{1}{MT_1}\,\frac{\varkappa}{\varkappa - 1}}. \qquad 8.3-9$$

If the pressure drop is above-critical (flow is sonic), then p_2/p_1 is to be replaced by the expression in Eq. 1.5—3, and the characteristic relationship is

$$q = k_7 p_1. \qquad 8.3-10$$

The production of wells tapping an *underground gas reservoir* can be described by the relationship

$$q = k_s(p_1^2 - p_2^2)^n \qquad 8.3-11$$

where, as distinct from the usual productivity relationship (cf. Section 3.1) p_1 means formation pressure and p_2 means wellhead pressure; k_s is a productivity index corresponding to this latter definition.

In the knowledge of the gas transmission system's elements, a mathematical-hydraulic model of the entire system may be constructed. In laying down the principles of modelling, the recognition of an analogy between gas flow in pipe networks and flow of electricity in electrical networks was extensively exploited. Kirchhoff's laws apply to gas flow, too. The first law applies to any node; the algebraic sum of gas flows entering and leaving the node is zero, that is

$$\sum_{i=1}^{m} q_i = 0 \qquad 8.3-12$$

where m is the number of NCEs meeting at the node. Gas flowing into the node is given the positive sign. By Kirchhoff's second law, for any loop in the high-pressure system, the algebraic sum of pressure drops, taken with signs corresponding to a consistent sense of rotation around the loop, is zero, that is,

$$\sum_{i=1}^{n} (p_1^2 - p_2^2)_i = 0. \qquad 8.3-13$$

where n is the number of NCEs in the loop, and p_1 and p_2 are, respectively, the head-end and tail-end pressures of said pipelegs, head and tail being taken with respect to the sense of rotation chosen. This relationship is also called the loop law. In low-pressure gas distribution networks, the compressibility of the gas is negligible and the loop law accordingly simplifies to

$$\sum_{i=1}^{n} (p_1 - p_2)_i = 0. \qquad 8.3-14$$

There are two fundamental types of gas transmission systems, loopless and looped.

8.3.2. Loopless systems

(a) Numerical methods

In a loopless system, NCEs joined by nodes form no closed loops anywhere in the system.

Figure 8.3—1 shows a hypothetical loopless system. Gas enters through node I and leaves through Nodes II, III and IV. Pressures and throughputs in such a system, assuming all NCEs to be pipelegs, are calculated as follows. In the knowledge of the gas volumes respectively injected into and taken out of the nodes, Eq. 8.3—12 furnishes the gas flows q_i in the

pipelegs. In possession of these latter, Eq. 8.3—1 yields pressure drops in the pipelegs and node pressures.

Example 8.3—1. Given the gas flows into and out of Nodes from I to IV of the pipeline shown in Fig. 8.3—1 and the parameters of pipelegs from *1* to *3* and the prescribed terminal pressure $p_{IV} = 18$ bars for Node IV; find the injection pressure p_I necessary to ensure the throughputs and the terminal pressure prescribed, and find the individual node pressures. The resistance factors calculated using Eq. 8.3—3 from the parameters of the pipelegs are listed in Column 3 of Table 8.3—1. The k_{1i}s have been replaced by k_is. Node throughputs are listed in Column 4, and the prescribed terminal pressure appears in the last row of column 9. In the possession of the node

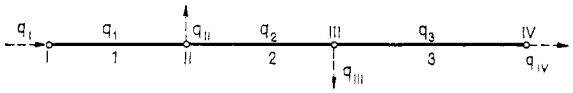

Fig. 8.3—1

throughputs, the pipeleg throughputs listed in Column 5 were calculated using node law 8.3—12. Column 7 states the pressure drops in the pipelegs. Now with p_{IV}, and hence, p_{IV}^2, given, one may find the remaining node pressures using the relationship

$$p_j^2 = p_{IV}^2 + \sum_{i=j}^{3} k_i \, q_i^2 \, ; \qquad 8.3-15$$

$$j = \text{III; II; I.}$$

The calculation reveals that an injection pressure of $p_I = 54.9$ bars is required to ensure a terminal pressure of $p_{IV} = 18$ bars.

The situation is somewhat more complicated if the injection and terminal pressures are fixed, and so are the injection and delivery rates at the intermediate nodes, and the problem is to find the maximum gas output that

Table 8.3—1

Node j	Pipeleg i	k_i $10^{10}\,\frac{N^2s^2}{m^{10}}$	q_j $\frac{m^3}{s}$	q_i $\frac{m^3}{s}$	$k_i q_i$ $10^{10}\,\frac{N^2s}{m^7}$	$k_i q_i^2$ $10^{10}\,\frac{N^2}{m^4}$	p_j^2 $10^{10}\,\frac{N^2}{m^4}$	p_j $10^5\,\frac{N}{m^2}$
1	2	3	4	5	6	7	8	9
I			+2.38				3008.5	54.9
	1	249.0		2.38	592.6	1410.4		
II			−0.38				1598.1	40.0
	2	145.0		2.00	290.0	580.0		
III			−0.80				1018.1	31.9
	3	482.0		1.20	578.4	694.1		
IV			−1.20				324.0	18.0

Table

Node	Pipeleg	k_i	q_j	$q_i^{(1)}$	$k_i q_i^{(1)}$	$k_i q_i^{(1)2}$
		$10^{10}\ \frac{N^2s^2}{m^{10}}$	$\frac{m^3}{s}$	$\frac{m^3}{s}$	$10^{10}\ \frac{N^2s}{m^7}$	$10^{10}\ \frac{N^2}{m^4}$
1	2	3	4	5	6	7
I						
	1	249.0		2.38	592.6	1410.4
II			−0.38			
	2	145.0		2.00	290.0	580.0
III			−0.8			
	3	482.0		1.20	578.4	694.1
IV						

estimation (1): $\Sigma k_i q_i^{(1)} = 1461.0\times10^{10}$

$q_{\mathrm{I}} = 2.38\ \mathrm{m^3/s} \rightarrow q_{\mathrm{IV}} = 1.2\ \mathrm{m^3/s}$

$$\Delta q = -\frac{(16\times10^5)^2 - (18.5\times10^5)^2}{2\times1461.0\times10^{10}} = 0.029 \approx 0.03$$

can be ensured at the delivery end of the line. The solution involves a successive approximation (Hain 1968) in the following steps: (i) Estimate the maximum throughput $q_1^{(1)}$ of the first pipeleg. (ii) Using Eq. 8.3—12, find the first-approximation throughputs $q_i^{(1)}$ of the individual pipelegs. (iii) In possession of these latter find the pressure drops in the pipelegs using Eq. 8.3—1. (iv) Using the relationship

$$p_j^2 = p_1^2 - \sum_{i=1}^{j-1} (p_1^2 - p_2^2)_i\ ; \qquad 8.3-16$$

$$j = \mathrm{II};\ \mathrm{III};\ \ldots,\ m$$

where m is the number of nodes, find the node pressures belonging to the $q_i^{(1)}$s calculated in the first approximation. (v) If the square of terminal pressure p_m deviates from the square of terminal pressure $p_m^{(1)}$ by more than the error permitted, then the throughputs determined in (ii) for the individual pipelegs are to be corrected using the expression $q_i^{(2)} = q_i^{(1)} + \Delta q$ where

$$\Delta q = -\frac{p_m^2 - p_m^{(1)2}}{2\sum_{i=1}^{n} k_i q_i^{(}}. \qquad 8.3-17$$

(vi) The procedure is repeated from Step (iii) on until the prescribed and calculated terminal pressures agree to within a prescribed tolerance.

Example 8.3—2. Find the maximum delivery rate at node IV in the pipeline characterized in the foregoing example, if $p_{\mathrm{I}} = 55$ bars and $p_{\mathrm{IV}} = 16$

p_j^2	p_j	$q_i^{(2)}$	$k_i q_i^{(2)}$	$k_i q_i^{(2)2}$	p_j^2	p_j
$10^{10}\ \frac{N^2}{m^2}$	$10^5\ \frac{N}{m^2}$	$\frac{m^3}{s}$	$10^{10}\ \frac{N^2 s}{m^7}$	$10^{10}\ \frac{N^2}{m^4}$	$10^{10}\ \frac{N^2}{m^4}$	$10^5\ \frac{N}{m^2}$
8	9	10	11	12	13	14
3025.0	55.0				3025.0	55.0
		2.41	600.1	1446.2		
1614.6					1578.8	39.7
		2.03	296.2	601.2		
1034.6					977.6	31.3
		1.23	592.9	729.2		
340.5	18.5				248.4	15.8

estimation (2): $\Sigma k_i q_i^{(2)} = 1489.2 \times 10^{10}$

$q_I = 2.41\ \text{m/s} \rightarrow q_{IV} = 1.23\ \text{m}^3/\text{s}$

$$\Delta q = -\frac{(16\times10^5)^2 - (15.8\times10^5)^2}{2\times1489.2\times10^{10}} = -0.0025$$

bars. — The main data of the solution are listed in Table 8.3 – 2. It shows that, at the given offtakes at intermediate nodes, the maximum delivery rate attainable at the delivery end of the pipeline is 1.23 m^3/s.

In the two approximations employed to solve the problem, the values of the k_is were unchanged although throughputs and tail-end pressures of the pipelegs were different. The reasons for this are, one, that flow is fully turbulent so that the friction factor is independent of the throughput-dependent Reynolds number and, two, the change in the mean pressures of the pipelegs is so slight that change in the compressibility factor z is negligible.

If there is a booster pump station installed somewhere along the pipeline, then the maximum throughput capacity of the pipeline can be calculated as follows (Hain 1968): Steps (i)—(iii) of the calculation are as above. (iv) In the knowledge of the gas throughput, intake pressure and installed compressor capacity, the output pressure of the pump can be determined for the node examined. (v) The tail-end pressure of the pipeline is calculated in the knowledge of the output pressure and of pressure drops in the individual pipelegs. (vi) If the calculated tail-end pressure differs from the prescribed one, pipeleg throughputs are once more corrected using the relationship $q_i^{(2)} = q_i^{(1)} + \Delta q$, but the correction itself is now calculated by means of the relationship

$$\Delta q = -\frac{p_m^2 - p_m^{(1)2}}{2\left[\dfrac{(p_2)_c^2 - (p_1)_c^2}{q_c} + \sum_{i=1}^{n} k_i q_i^{(1)}\right]} \qquad 8.3-18$$

where $(p_1)_c$ and $(p_2)_c$ are the intake and discharge pressures of the compressor, respectively, and q_c is compressor output.

(b) Graphical methods

A quick and simple graphical method for solving problems involving the throughput and pressure parameters of gas transmission lines, based on diagrams, has been proposed by van den Hende (1969).

The first step is to plot the family of curves $\Delta p = f(p_1)_q$, resembling Fig. 8.3–2 for the pipeline examined, with both axes of coordinates calibrated in the same units. The plots are calculated using the equations

$$\Delta p = p_1 - p_2 = p_1 - \sqrt{p_1^2 - kq^2}. \qquad 8.3-19$$

Here, p_2 is expressed using Eq. 8.3–1. The k factor in Eq. 8.3–19 is identical with the k_1 figuring in Eq. 8.3–3. The values of λ and z figuring there are functions of p and q. Plotting the family of curves may be simplified, however, by assuming for the purposes of approximate calculations that λ and z are constant for any value of p and q. Van den Hende has developed a procedure for the calculation of k out of a function $k = Cl$, where C can be read off a table as a function of pipe size d_i. Whichever way k is determined, the individual curves of the family may be constructed by the graphical procedure illustrated in Fig. 8.3–3. The value of p_o is furnished by Eq. 8.3–1 after the substitution $p_2 = 0$, that is,

$$\Delta p_o = q\sqrt{k}\,.$$

Plotting any point of the curve is performed in a manner similar to the construction starting from point A. Equation 8.3–1 holds for any point of this curve. For instance, it is clear on inspection that the hypotenuse of triangle OAB is precisely equal to the abscissa of point P, and that, in the triangle,

$$p_1^2 = p_2^2 + kq^2\,.$$

In possession of a family of curves characterized by a given k, any one of the three parameters p_1, p_2 and q of the pipeline can be determined rapidly in possession of the other two.

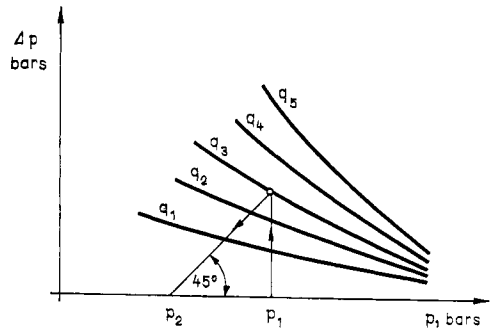

Fig. 8.3–2 Graphical procedure, after van den Hende (1969)

Example 8.3—3. Find the head-end pressure p_I required to ensure the tail-end pressure $p_{IV} = 18$ bars in the pipeline schematically shown as Fig. 8.3—1, under the conditions stated in Example 8.3—1. — Figure 8.3—4 illustrates the family of curves plotted using Eq. 8.3—19. The manner of constructing the head-end pressure is shown by the full line in the Figure. The resulting head-end pressure is $p_I = 55$ bars. This graphical method lends itself well to the solution of numerous other problems, too.

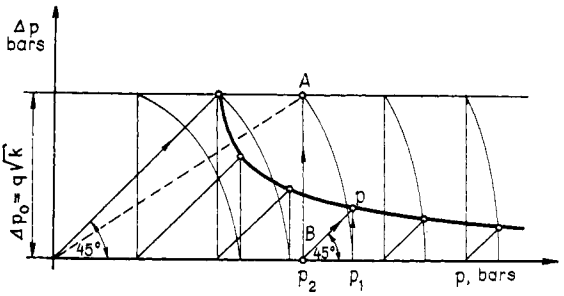

Fig. 8.3—3 Graph $\Delta p = f(p)$, after van den Hende (1969)

Example 8.3—4. In the pipeline characterized in the foregoing example, we want to raise the pressure at Node III from 31.9 to 35 bars. What is the pressure increment required at the head end, and what will the pressures at Nodes II and IV be? — The solution of the problem is shown in dashed line in Fig. 8.3—4. The result is $\Delta p_I = 1{,}5$ bar for the required pressure increment at the head end, and 42.7 and 24.3 bars, respectively for the resulting pressures at Nodes II and IV.

8.3.3. Looped systems

The first procedure for modelling a low-pressure looped network was developed by Cross (1936); it was adapted with some modifications also to high-pressure systems (Hain 1968). Let us illustrate the application of this method on the loop shown as Fig. 8.3—5. The gas flows into and out of the nodes are known, and so is pressure p_I at Node I. We are to find the gas throughputs of the indivual pipelegs, as well as the pressures in the remaining nodes. The solution is based on the following consideration. Taking clockwise flow as positive, let us assume a first-approximation value $q_1^{(1)}$ for the throughput of pipeleg *1*. Let us then use the node law to find the gas throughputs $q_i^{(1)}$, whose signs will be according as flow is clockwise or counterclockwise. In the steady state, the loop law (8.3—13 or 8.3—14) will have to apply. If it is assumed that the first-approximation values of throughputs in the individual pipelegs differ by Δq from the actual throughput, then

$$\sum_{i=1}^{n} k_i (q_i^{(1)} + \Delta q)\,|q_i^{(1)} + \Delta q| = 0\,,$$

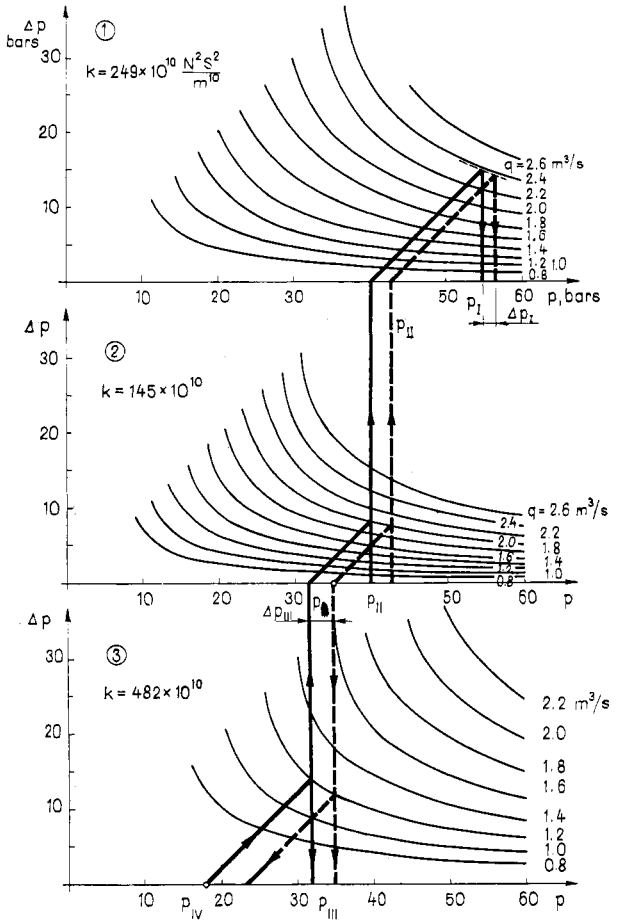

Fig. 8.3 – 4 Throughput and pressure distribution in the pipeline specified in Fig. 8.3 – 1

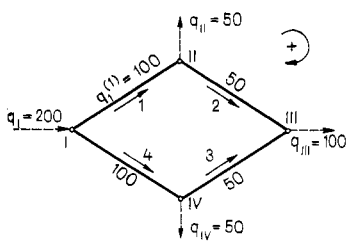

Fig. 8.3 – 5 Looped transmission system to Cross' method

where n is the number of node-connecting elements (pipelegs). By this relationship, the correction is

$$\Delta q = -\frac{\sum_{i=1}^{n} k_i |q_i^{(1)}| q_i^{(1)}}{2 \sum_{i=1}^{n} k_i |q_i^{(1)}|} \qquad 8.3-20$$

provided $|\Delta q| \ll q_i$; the second-approximation values of the gas throughputs in the individual pipelegs can now be calculated as

$$q_i^{(2)} = q_i^{(1)} + \Delta q. \qquad 8.3-21$$

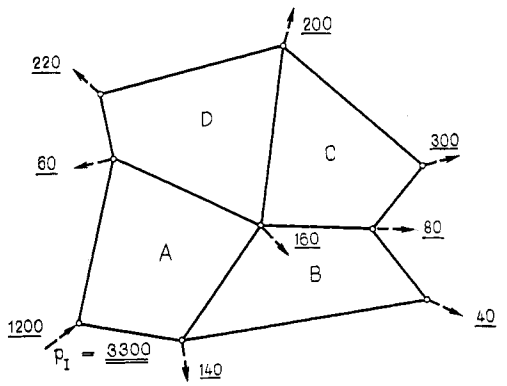

(a)

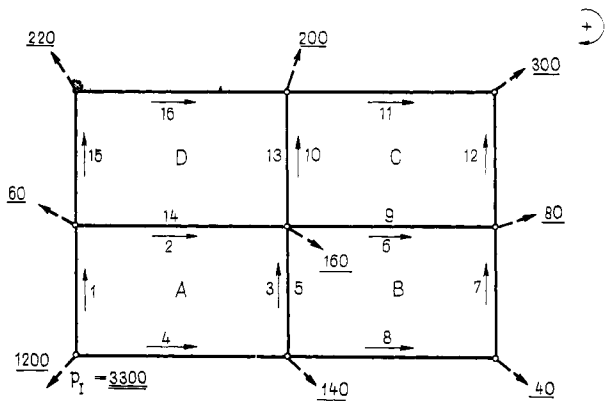

(b)

Fig. 8.3—6 Layout and hookup of low-pressure looped gas supply system

Table

Loop	Pipeleg	d_i	l_i	k_i	$q_i^{(j)}$	$q^{(1)}$	$k_i\|q_i\|^{(1)}$
		m	m	$\frac{10^4\ \mathrm{Ns^2}}{\mathrm{m^8}}$	$\mathrm{m^3/h}$	$10^{-2}\ \mathrm{m^3/s}$	$\frac{10^4\ \mathrm{Ns}}{\mathrm{m^5}}$
1	2	3	4	5	6a	6b	7
A	1	0.3071	450	0.1240	700	19.444	0.0241
	2(14)	0.1541	420	4.5759	200	5.556	0.2542
	3(5)	0.1541	370	4.0311	−200	− 5.556	0.2240
	4	0.2589	280	0.1917	−500	−13.889	0.0266
	$\sum_{i=1}^{4}$						0.5289
B	5(3)	0.1541	370	4.0311	200	5.556	0.2240
	6(9)	0.1023	290	28.087	200	5.556	1.5604
	7	0.1023	240	23.245	−120	−3.333	0.7748
	8	0.1023	660	63.923	−160	−4.444	2.8410
	$\sum_{i=5}^{8}$						5.4002
C	9(6)	0.1023	290	28.087	−200	−5.556	1.5604
	10(13)	0.1541	480	5.2296	40	1.111	0.0581
	11	0.1023	480	46.489	60	1.667	0.7748
	12	0.1023	220	21.308	−240	−6.667	1.4205
	$\sum_{i=9}^{12}$						3.8138
D	13(10)	0.1541	480	5.2295	− 40	−1.111	0.0581
	14(2)	0.1541	420	4.5759	−200	−5.556	0.2542
	15	0.3071	180	0.0496	440	12.22	0.0061
	16	0.2051	500	1.1859	220	6.111	0.0725
	$\sum_{i=13}^{16}$						0.3909

If after the kth successive approximation Δq is within the tolerance admitted, then the node pressures can be calculated using the relationship

$$p_j^2 = p_1^2 - \sum_{i=1}^{j-1} k_i |q_i^{(k)}| q_i^{(k)}; \qquad 8.3-22$$

$$j = \mathrm{I};\ \mathrm{II};\ \ldots$$

for a high-pressure network or

$$p_j = p_\mathrm{I} - \sum_{i=1}^{j-1} k_i |q_i^{(k)}| q_i^{(k)} \qquad 8.3-23$$

for a low-pressure network; k equals k_1 in Eq. 8.3–3 in the first case, and k_2 in Eq. 8.3–6 in the second.

If the system is composed of several loops, then, after a first-approximation estimation of the throughputs in the individual pipelegs, one calculates a Δq for each loop, and then performs the correction of the pipelegs'

$\Delta p_i = k_i q_i^{(1)} \lvert q_i^{(1)} \rvert$	Δq	$q_i^{2)}$	...	$q_i^{(s)}$	$q_i^{(s)}$	$\Delta p = k_i q_i^{(s)} \lvert q_i^{(s)} \rvert$	p_{Ii}	p_{IIi}
$\frac{N}{m^2}$	$10^{-2}\ \frac{m^3}{s}$	$10^{-2}\ \frac{m^3}{s}$		$10^{-2}\ \frac{m^3}{s}$	m^3/h	$\frac{N}{m^2}$	$\frac{N}{m^2}$	$\frac{N}{m^2}$
8	9	10		11a	11b	12	13	14
46.87		19.192	...	20.960	754.6	54.47	3300	3246
141.23	—0.252	4.076	...	4.532	163.2	93.98	3246	3152
— 124.42		— 6.298	...	— 5.486	—197.5	—121.30	3152	3273
— 36.99		—14.141	...	—12.373	—445.4	— 29.35	3273	3302
26.70						— 2.20		
12.42		6.298	...	5.486	197.5	121.30	3273	3152
866.89	0.490	3.846	...	4.353	156.7	532.14	3152	2619
— 258.27		— 2.843	...	— 1.888	— 68.0	— 82.81	2619	2702
1262.7		— 3.954	...	— 2.999	108.0	—574.75	2702	3277
— 529.64						— 4.12		
— 866.89		— 3.846	...	— 4.353	—156.7	—532.14	2619	3152
6.46	2.200	2.083	...	1.220	43.9	7.79	3152	3144
129.14		3.867	...	4.315	155.3	865.76	3144	2278
— 947.0		— 4.466	...	— 4.018	144.6	—343.98	2278	2622
—1678.3						— 2.58		
— 6.46		— 2.083	...	— 1.220	— 43.9	— 7.79	3144	3152
— 142.23	1.228	— 4.076	...	— 4.532	—163.2	— 93.98	3152	3246
7.41		13.450	...	14.762	531.4	10.81	3246	3235
44.29		7.339	...	8.651	311.4	88.74	3235	3146
95.99						— 2.22		

throughputs loop after loop. The pipelegs common to two loops are corrected using the Δqs determined for both loops. Let us illustrate this procedure by an example referring to a low-pressure network.

Example 8.3—5. Given the gas flows into and out of the nodes of the network shown as Fig. 8.3—6a, and given the pressure $p_{I(1)} = 3300\ N/m^2$ of node $I_{(1)}$; find the gas throughputs of the individual pipelegs, and the individual node pressures. The loops are considered to be balanced if the condition $\left| \sum_{i=1}^{n} \Delta p_i \right| < 5\ N/m^2$ is satisfied. A working model of the network is shown as part (b) of Fig. 8.3—6. The numbering, sizes and length of the pipelegs composing the loops in the Figure are given in Columns 2—4 of Table 8.3—3. The pressure drops in the individual pipelegs are calculated using the relationship

$$\Delta p_i = k_i \lvert q_i \rvert q_i \qquad 8.3—24$$

derived from Eq. 8.3—4; k_i is furnished by Eq. 8.3—6, with $p_n = 1.014 \times 10^5$ N/m², $T_n = 288.2$ K, $M = 16.03$ kg/kmole, $\bar{T} = 283$ K, and $\bar{\lambda}$ is obtained using Eq. 1.2—5. After substitutions,

$$k_i = 5.079 \times 10^{-3} \frac{l_i}{d_i^{5.333}}.$$

The values calculated in this way are listed in Column 5. Column 6 of the Table lists the first-approximation throughputs of the individual pipelegs, with clockwise rotation regarded as positive. In estimating these throughputs, the circumstance that the condition implicit in Eq. 8.3—12 must hold for each node separately was taken into due account. The pressure drops in Column 8 were calculated using Eq. 8.3—24. The Δqs for the individual loops were determined from Eq. 8.3—20; for instance, in loop A,

$$\Delta q_A = -\frac{26.70}{2 \times 0.5289 \times 10^4} = -0.252 \times 10^{-2} \text{m}^3/\text{s}.$$

The summed data of Column 8 show that $\left| \sum_{i=1}^{4} \Delta p_i \right|$ exceeds in each loop the tolerance of 5 N/m², so that the values listed in Column 6b have to be corrected. In the pipelegs which belong to one loop only, the corrected throughputs are supplied by Eq. 8.3—21. In the pipelegs common to two loops, the throughputs must of course be the same (Column 10). The corrected throughputs are calculated as shown in the example below. By the values for pipelegs *2* and *14* in Column 6b, the first approximation throughput was 5.556×10^{-2} m³/s with signs according to the sense of rotation. The absolute value of the corrected throughput, calculated by means of Eq. 8.3—21 but not stated in the Table, is 5.304×10^{-2} m³/s in pipeleg *2*. The throughput of pipeleg *14* is equated with this value, and then corrected using the correction for loop D and Eq. 8.3—21. The value obtained is -4.076×10^{-2} m³/s, and accordingly the throughput in leg *2* is 4.076×10^{-2} m³/s. It is these values that are entered into the corresponding rows of Column 10. Iteration is pursued with the q_is of Column 10. After seven steps of iteration, not given in detail, one obtains the last-step data and the final results listed in Columns 11—14. Clearly, by the data in Column 12, $\left| \sum_{i=1}^{n} \Delta p_i \right|$ is in every case within the tolerance of 5 N/m². The data in Columns 13 and 14 are the $p_{\text{I}i}$s and $p_{\text{II}i}$s, the pressures at the head and tail ends, respectively, of the individual pipelegs, based on the pressure drop data in Column 12 and on the condition of $p_{\text{I}(1)} = 3300$ N/m² at the node common to pipelegs *1* and *4*.

The main advantage of the Cross method is its simplicity, whereas its main drawback is the slowness of the convergence, which renders this method uneconomical in many applications. In order to eliminate these drawbacks, Renouard developed a variant of the Cross method (Société . . . Manuel 1968). The Renouard method is suited for the modelling of steady-state operation in not-too-complicated looped networks. The method was generalized by Pernelle for networks of any size (Société . . . Manuel 1968)

The essence of this latter method is as follows. In the foregoing example we required a throughput correction Δp for each loop in each step of iteration. Let us denote the throughput correction to be calculated by Δq_A in the case of loop A, Δq_B in the case of loop B, etc. The throughput correction of the pipeleg(s) common to loops A and B is, then, $(\Delta q_A - \Delta q_B)$, that of the pipelegs common to loops B and C, $(\Delta q_B - \Delta q_C)$, etc. — Equation 8.3—20 permits us to write up for the n loops n linear equations in the n throughput corrections Δq_A, Δq_B, Δq_C, etc. The corrections are furnished by the solution of this system of equations. After applying the corrections to the throughputs, the values obtained are checked to see whether they satisfy loop law 8.3—13; if the aggregate pressure drops of the loops exceed the prescribed tolerance, then the procedure is repeated. This method furnishes, according to its authors, a result of sufficient accuracy in two or three steps even if the first estimates of the individual throughputs of the pipelegs are rather wide of the mark.

Stoner's method for solving looped networks is based on the node continuity equation (Stoner 1970). It has the advantage that, whereas the Cross method can be used to establish throughput and pressure maps of the network only, the Stoner method will furnish any parameter (pipe size in a leg, compressor horsepower required, number of storage wells, size of pressure-reducing choke, etc.) of the complex system. It is, however, significantly more complicated than the previously mentioned methods, and it requires much more computer time. — The way of constructing the model is illustrated in Fig. 8.3—7. Node *11*, selected as an example, receives gas

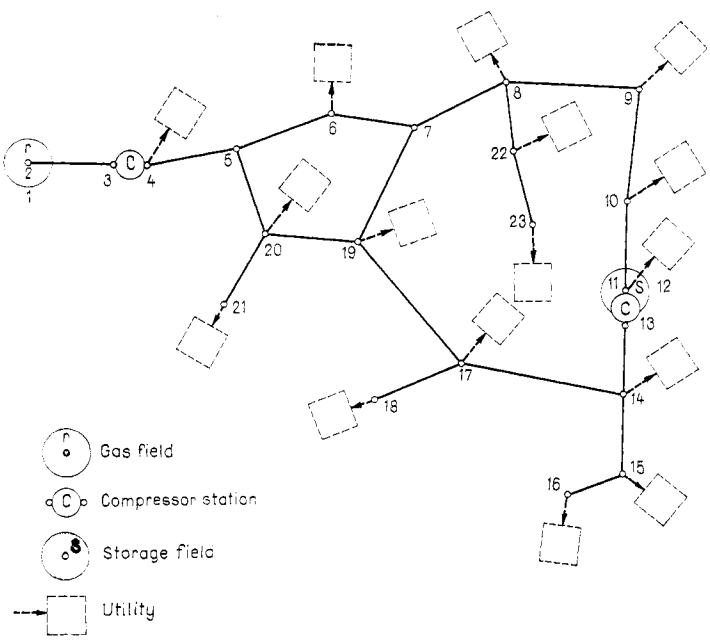

Fig. 8.3—7 Regional gas transmission system

from underground storage facility (*12—11*) and pipeleg (*10—11*), and delivers gas into the intake of pump (*13—11*), and into the consumer supply circuit directly attached to the node. By this model, the node equation 8.3—12 can be given the form

$$F_{11} = (q_{12-11})_s - (q_{13-11})_c + (q_{10-11})_p - q_{o11} = 0 \qquad 8.3-25$$

where suffixes s, p and c respectively refer to storage, pipeleg and compressor, and q_{o11} is the flow of gas out of node *11*. Flow into the node is positive. The measure of imbalance at the node is F_{11}; its value is zero if the node is balanced, that is, if the condition $|F_j| < \varepsilon$ is satisfied, where ε is the tolerance. Introducing into this Equation the Relationships 8.3—1, —7 and —11, we get

$$F_{11} = J_{12-11}(|p_{12}^2 - p_{11}^2|)_n S_{12-11} - \frac{p_{13-11}}{k_3\left(\frac{p_{13}}{p_{11}}\right)^{k_4} + k_5} + \\ + \frac{(|p_{10}^2 - p_{11}^2|)^{0.5}}{(k_1)_{10-11}^{0.5}} S_{10-11} - q_{o11} = 0 \qquad 8.3-26$$

where $S_{i,j}$ is a sign factor accounting for flow direction:

$$S_{i,j} = \text{sign}\,(p_i - p_j) = \begin{cases} +1 \text{ if } p_i \geq p_j \\ -1 \text{ if } p_i < p_j \end{cases}.$$

Writing up in a similar fashion n equations of continuity for the n nodes of the system, one obtains the non-linear system of Equations constituting the mathematical model of the system in the steady state.

The equations contain node pressures, inputs/outputs and the parameters of the NCEs (node connecting elements), altogether $(2n + m)$ parameters, where n is the number of nodes and m is the number of NCEs. The model of n equations will in principle yield any n unknowns of the $(2n + m)$ parameters, if the remaining $(n + m)$ parameters are given. These equations, similar to Eq. 8.3—26, can thus be written in the form

$$F_j(x_1, x_2, \ldots x_n) = 0 \qquad 8.3-27$$
$$j = 1, 2, \ldots, n.$$

The only criterion in choosing the n unknowns to be calculated is that the continuity equations of the type 8.3—26, written up for the nodes, must remain mutually independent. Since the value of the nodal gas throughput is independent in $(n - 1)$ equations only, at least one of the values q_{oj} must be known. It is likewise necessary to state at least one node pressure.

The solution of the non-linear system of Equations 8.3—27 constituting the mathematical model of the network may be achieved by the Newton—Raphson technique. The essence of this method is that it provides linear relationships for correcting the initial, estimated values of the unknowns, and said relationship of correction ensures that the successive steps of

iteration make the system approach the solution. Let the value of the ith unknown, denoted x_i, be $x_i^{(k)}$ after the kth step of iteration; then

$$x_i^{(k+1)} = x_i^{(k)} + \Delta x_i^{(k+1)};\ i = 1, 2, \ldots, n \qquad 8.3-28$$

where the Δx_is are furnished in each step of iteration by the solution of the linear system of equations

$$\sum_{i=1}^{n} \frac{\partial F_j}{\partial x_i} \Delta x_i = -F_j; \qquad j = 1, 2, \ldots, n. \qquad 8.3-29$$

The $\partial F_j/\partial x_i$s are the values of the derivatives of the node continuity equations taken at the x_is calculated in the foregoing step of iteration. The linear system of Equations 8.3—29 may be solved by direct elimination. The Newton—Raphson method requires that the initial values $x_i^{(1)}$ of the unknowns x_i be estimated. The convergence behaviour of the iteration will depend to a significant degree on the goodness of these estimates, even in a fairly simple system. A suitable rate of convergence may be ensured, according to Stoner's proposition, in the following way. Introducing the acceleration factor α_i, Eq. 8.3—28 can be written in the form

$$x_i^{(k+1)} = x_i^{(k)} + \Delta x_i^{(k+1)} \alpha_i . \qquad 8.3-30$$

The value of α_i can be expressed in terms of the actual and the foregoing corrections Δx_i as follows. Let

$$A_i = \frac{\Delta x_i^{(k+1)}}{\Delta x_i^{(k)}};$$

if	$A_i \leq -1$,	then	$\alpha_i = 0.5 \mid A_i \mid$;
if	$-1 < A_i < 0$,	then	$\alpha_i = 1.0 - 0.5 \mid A_i \mid$;
if	$0 < A_i < 1$,	then	$\alpha_i = 1.0 + 2.0 \mid A_i \mid$;
if	$A_i \geq 1$,	then	$\alpha_i = 3.$

In the first two steps of iteration, where divergence is most likely to occur, it is best to put $\alpha_i = 0.5$ to ensure convergence. In the subsequent steps, the values of α_i are determined as above in every other step; in the steps in between, α_i is put equal to 1.0. This method ensured convergence in every case and gave results of satisfactory accuracy after 6—10 steps.

Stoner (1971, 1972), in a development of the above method, gave a procedure for determining the 'sensitivity' of the system in steady-state operation. The purpose of the calculation is in this case to find out in what way some change(s) in some parameter(s) of the system affect the remaining parameters. For instance, what changes in input pressures and flow rates, or compressor horsepower, are to be effected in order to satisfy a changed consumer demand? Schematically the method can be outlined as follows. — Let y_i denote those n parameters whose changes we are interested in, after other m parameters of the system, denoted x_i in their turn, have been changed. In this notation, the non-linear system of equations resembling

Eq. 8.3—26, constituting the model of the system, can be written in the form

$$F_j(y_1, y_2, \ldots, y_n; x_1, x_2, \ldots, x_m) = 0 \qquad 8.3-31$$
$$j = 1, 2, \ldots; n.$$

The Taylor series expansion of the function F_j, with all but the linear terms dropped, is

$$\sum_{i=1}^{n} \frac{\partial F_j}{\partial y_i} \mathrm{d}y_i + \sum_{i=1}^{m} \frac{\partial F_j}{\partial x_i} \mathrm{d}x_i = 0\,; \quad j = 1, 2, \ldots, n. \qquad 8.3-32$$

Each one of the two sets of derivatives, $\partial F_j/\partial y_i$ and $\partial F_j/\partial x_i$, formally identical with the derivatives figuring in Eq. 8.3—29, can be regarded as forming a matrix:

$$\mathbf{J} = \begin{bmatrix} \frac{\partial F_1}{\partial y_1} & \cdots & \frac{\partial F_1}{\partial y_n} \\ \vdots & & \vdots \\ \frac{\partial F_n}{\partial y_1} & \cdots & \frac{\partial F_n}{\partial y_n} \end{bmatrix};$$

$$\mathbf{C} = \begin{bmatrix} \frac{\partial F_1}{\partial x_1} & \cdots & \frac{\partial F_1}{\partial x_m} \\ \vdots & & \vdots \\ \frac{\partial F_n}{\partial x_1} & \cdots & \frac{\partial F_n}{\partial x_m} \end{bmatrix}.$$

Using these identities, Eq. 8.3—32 may be rewritten in matrix notation as

$$\mathbf{J}\,\mathrm{d}y + \mathbf{C}\,\mathrm{d}x = 0 \qquad 8.3—33$$

which after rearranging becomes

$$\mathrm{d}y = -\mathbf{J}^{-1}\mathbf{C}\,\mathrm{d}x$$

where $\mathbf{J}^{-1}$ is the inverse of $\mathbf{J}$. The matric resulting from the multiplication $-\mathbf{J}^{-1}\mathbf{C}$ is the so-called sensitivity matrix of the system, to be denoted by the symbol $[\mathrm{d}_y/\mathrm{d}_x]$. It is a measure of change in the parameters y_i resulting from unity changes in the parameters x_i, provided that the node continuity equation 8.3—12 is satisfied for every node. It suffices to determine the sensitivity matrix just once to be able to determine by a simple matrix multiplication the change in the parameters y_i of the system, resulting from any change in the parameters x_i, represented by the vector Δx:

$$\Delta y = \left[\frac{\mathrm{d}_y}{\mathrm{d}_x}\right] \Delta x\,. \qquad 8.3-34$$

8.4. Transient flow in pipeline systems

Flow parameters in gas transmission pipelines are usually time-dependent, the main reason for which is the variation in demand, as a function of a variety of factors. If the fluid flowing in the pipe were incompressible, Newtonian, then the change in throughput would take place at the same instant and would be of the same magnitude at any pipeline section, including the head and the tail end. Such transient flow could, then, at any instant be described by the equations of steady-state flow over the whole length of the pipeline. If, however, demand at the delivery end of a pipeline conveying compressible gas changes then it takes a time Δt for the resulting pressure reduction to make itself felt at the head end of the pipeline. The equations of steady-state flow will, then, apply to infinitesimal lengths of pipeline only. Still, even the equations of flow in a complex system made up of pipelegs of considerable length may be derived from these fundamental relationships. It has been primarily thanks to the electronic computer that several increasingly more accurate procedures for modelling gas flow in complicated pipeline systems have been able to be developed in the last decade and a half.

8.4.1. Fundamental relationships

The relationships describing flow in pipelines of finite length may be derived from four fundamental relationships; any differences in these are merely matters of formulation. The equation of continuity is

$$\frac{\partial q_m}{\partial x} + \frac{\partial(\varrho A_i)}{\partial t} = 0. \qquad 8.4-1$$

The equation of energy or of motion is the transient form, accounting for the change of parameters in time, of Eq. 1.2—1:

$$\frac{\partial p}{\partial x} + \varrho g \sin \alpha + \frac{\lambda v^2 \varrho}{2 d_i} + \varrho \frac{\partial v}{\partial t} = 0. \qquad 8.4-2$$

The equation of state for a gas flow regarded as isothermal is, by Eq. 8.1—1

$$\frac{p}{\varrho} = z \frac{R}{M} T .$$

The fourth fundamental relationship

$$z = \mathrm{f}(p)_T ,$$

has several solutions employed in practice, one of which is Eq. 8.1—9. If z is replaced by its average value and considered constant, then the number of fundamental equations reduces to three, and Eq. 8.1—1 may be written in the simpler form

$$\frac{p}{\varrho} = B^2 , \qquad 8.4-3$$

where B is the isothermic speed of sound. Eqs 8.4—1 and 8.4—3 imply

$$F_1 = \frac{B^2 \partial q_m}{A_i \partial x} + \frac{\partial p}{\partial t} = 0 \qquad 8.4—4$$

where mass flow is

$$q_m = \varrho A_i v = \frac{p}{B^2} A_i v \,.$$

By Eqs 8.4—2, 8.4—3 and the above definition of q_m,

$$F_2 = \frac{1 \partial p^2}{2 \partial x} + \frac{p \partial q_m}{A_i \partial t} + \frac{p^2 g}{B^2} \sin \alpha + \frac{\lambda B^2 q_m |q_m|}{2 d_i A_i^2} = 0. \qquad 8.4—5$$

Equations 8.4—4 and —5 constitute a system of non-linear partial differential equations; then, on the assumption that $\bar{z}$ = constant, describe transient flow in the pipeline system.

8.4.2. Flow in pipelines

(a) Matching the system to variable consumer demand

There are two frequently-employed ways of adapting flow in pipelines to the (usually daily) fluctuation of consumer demand. It holds for both cases that over the period of fluctuation (which we shall henceforth equate with one day) the gas quantity injected into the pipeline equals the gas offtake, that is, the consumption out of the line. In the first case, the hourly injection of gas into the pipeline is constant, say q_{in} in standard volume units. At the delivery end of the pipeline, pressure varies between the minimum required at the head end of the consumer supply network, p_{2min}, and the peak pressure p_{2max}, occurring when demand is at a low end. This setup has the advantage that the rate of injecting gas into the pipeline is constant, requiring no regulation within one day. The difference between the constant input and the fluctuating offtake is taken up by the pipeline acting as a buffer storage facility. The drawback of this setup is that a significant portion of the pressure energy in the gas is dissipated by a throttle at the delivery end, since over most of the day the tail-end pressure of the pipeline exceeds the p_{2min} required by the consumer supply network. Energy loss is minimized in certain instances by making the gas pass through a gas turbine rather than a pressure reducer, and letting the turbine drive an electric generator. The output of this latter is fed to the grid. An approximate designing of the pipeline may be performed by the following procedure of Smirnov and Shirkovsky, slightly modified (Szilas 1967).

Equation 1.2—7 may be restated in the following simple form:

$$q = k \sqrt{\frac{p_1^2 - p_2^2}{\bar{z}}} \,. \qquad 8.4—6$$

Let us point out that, as opposed to the factor k_1 in Eq. 8.3—2, the k occurring here does not include the compressibility factor $\bar{z}$. By Eq. 8.4—6,

$$p_1 = \sqrt{p_2^2 + \frac{q^2 \bar{z}}{k^2}}\,, \qquad 8.4-7$$

and, introducing the expression $p_1/p_2 = R_p$,

$$p_1 = \frac{q R_p \sqrt{\bar{z}}}{k \sqrt{R_p^2 - 1}}. \qquad 8.4-8$$

Likewise by Eq. 8.4—6,

$$p_2 = \sqrt{p_1^2 - \frac{q^2 \bar{z}}{k^2}} \qquad 8.4-9$$

and, putting $p_1/p_2 = R_p$,

$$p_2 = \frac{q \sqrt{\bar{z}}}{k \sqrt{R_p^2 - 1}}. \qquad 8.4-10$$

Introducing the expressions of p_1 and p_2 in Eqs 8.4—8–10 into the Eq. 1.2—26 for the mean pressure, and rearranging, we get

$$\frac{3pk}{2q\sqrt{\bar{z}}} = \frac{R_p^2 + R_p + 1}{(R_p + 1)\sqrt{R_p^2 - 1}}. \qquad 8.4-11$$

Figure 8.4—1 is a plot of the expression $3pk/2q\sqrt{\bar{z}}$ v. R_p as furnished by Eq. 8.4—11.

The above-given relationships permit us to find out whether the maximum pressure $p_{1\max}$ that can be ensured at the head end of the pipeline is sufficient to satisfy consumer demand, provided injection rate of gas into the pipe-

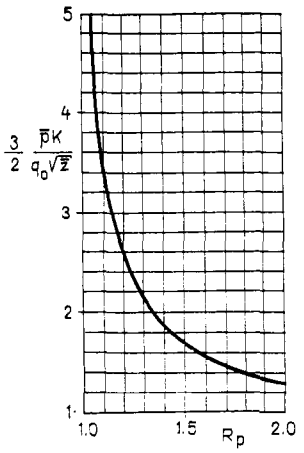

Fig. 8.4—1 For determining the buffer action of a pipeline (I), after Smirnov and Shirkovsky (1957) and Szilas (1967)

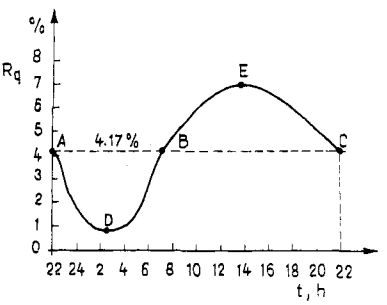

Fig. 8.4—2 For determining the buffer action of a pipeline (II), according to Smirnov and Shirkovsky (1957) and Szilas (1967)

line is uniform. Calculation proceeds as follows. (i) Gas consumption is plotted v. time t on the basis of daily consumption records. Figure 8.4—2 shows the daily fluctuation of R_q, the percentage hourly consumption referred to daily consumption. The input into the pipeline per hour is 1/24th of the daily consumption, that is,

$$\bar{q} = \frac{1}{24} \int_{t=0}^{24} q(t)\,\mathrm{d}t\,.$$

The line parallel to the abscissa axis, having ordinate $\bar{q}$, intersects the curve at points A, B and C. In segment $A-B$, consumption is less than $\bar{q}$; that is, gas accumulates in the pipeline. In segment $B-C$, the gas thus accumulated is used to cover higher-than-average demand. (ii) Gas flow into the pipeline is precisely equal to demand at point A. The gas reserve in the pipeline has dropped to zero at that point; that is, pressure at the tail end of the pipeline must at that instant be $p_{2\min}$, which is the least pressure required at the head end of the consumer supply system. Applying in an approximation the relationship for steady-state flow, we get by Eq. 8.4—7 for pressure at the head end of the pipeline at this same instant

$$p_1 = \sqrt{p_{2\min}^2 + \frac{q^2 \bar{z}}{k^2}}$$

where $\bar{z}$ can be determined by iteration using the given $\bar{T}$ and the p calculated from p_1 and $p_{2\min}$, applying Eq. 1.2—26. The mean pressure in the pipeline is, then,

$$\bar{p} = \frac{2}{3}\left(p_1^2 + \frac{p_{2\min}^2}{p_1 + p_{2\min}}\right).$$

For the standard-state volume of gas in the pipeline, the general gas law furnishes

$$V_{OA} = \frac{T_n \bar{p} A_i l}{p_n \bar{z} T}\,. \qquad 8.4-12$$

(iii) The area embraced by curve segment $A-D-B$ and line segment $A-B$ is determined by planimetering. Multiplying this by the scale of the diagram, we get the volume V_{OAB} of gas stored up in the slack-demand period. (iv) Said stored-up volume will be a maximum at the instant corresponding to B, and hence, the head- and tail-end pressures p_1 and p_2, respectively, of the pipeline will also be maximal at that instant. The mean pressure in the pipeline, corrected by $\bar{z}$, is at that instant

$$\frac{\bar{p}}{\bar{z}} = \frac{p_n}{T_n} V_{O\mathrm{al}} \frac{T}{A_i l}, \qquad 8.4-13$$

where $V_{O\mathrm{al}} = V_{OA} + V_{OAB}$. — From $\bar{p}/\bar{z}$, $\bar{p}$ and $\bar{z}$ may be determined by successive approximation. (v) The next step is to calculate the value of the expression $3\bar{p}k/2q\sqrt{\bar{z}}$ and to read the corresponding R_p off Diagram

8.4—1. In the possession of this latter, Eq. 8.4—10 may be used to furnish p_2, whereupon $p_1 = R_p p_2$. If the technically feasible maximum pressure at the head end of the pipeline is $p_{1\max}$, then the quantity of gas V_{OAB} stored up in the pipeline during the period $A-B$ will suffice to cover the excess demand in the period $B-C$, if $p_1 = p_{1\max}$.

The second way to satisfy fluctuating consumer demand is to inject into the pipeline gas at varying pressures and rates of injection, so as to ensure an unvaried tail-end pressure p_2 in the pipeline, equal to what is required by the consumer supply network. This, of course, can be realized only if the variations in demand in the supply circuit can be predicted to a fair degree of accuracy. The problem can be solved making use of the relationships given in Section 8.1—4. In the following we shall describe the principle of the Batey—Courts—Hannah method of solution and discuss the conclusions that can be drawn from a numerical example (Batey et al. 1961).

Gas-consumption variations in time can be represented by a Fourier function. Figure 8.4—3 shows the graph of such a function, $q_2 = \mathrm{f}(t)$. In possession of this graph, and of the constant pressure p_2 prescribed, we may, starting from fundamental relationships, calculate functions of gas flow rate and pressure v. time, step by step for various pipeline sections, proceeding backward along the line. Such functions referring to the head end of the pipeline are illustrated by graphs $q_1 = \mathrm{f}'(t)$ and $p_1 = \mathrm{f}''(t)$ shown in Fig. 8.4—3. The group of diagrams in Fig. 8.4—4 has been prepared on the basis of several similar diagrams. These permit us to conclude upon several characteristics of transient flow. The six top diagrams are plots of each variable v. the frequency of the demand wave. Each curve in parts (a), (c) and (e) of the Figure shows the output flow-rate wave to have a lower amplitude q_{ao} than the input flow-rate wave (whose ampli-

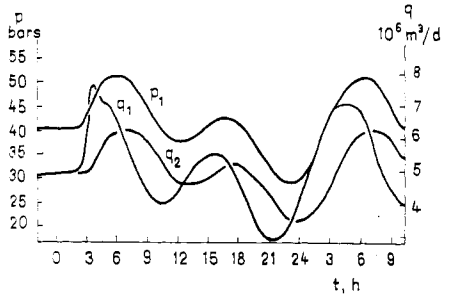

Fig. 8.4—3 Transient flow (I), after Batey et al. (1961)

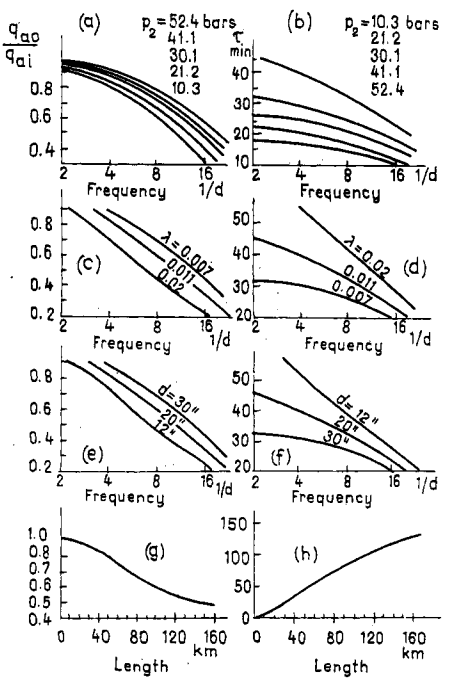

Fig. 8.4—4 Transient flow (II), after Batey et al. (1961)

tude is q_{ai}); damping increases as the frequency. For a given frequency, the amplitude ratio is the less, that is, damping is the stronger, the lower the tail-end pressure p_2 (part (a) of the Figure), the lower the friction factor λ, and the less the pipe size d_i. Each curve in parts (b), (d), and (f) of the Figure shows the phase shift of the demand wave to be the less, that is, phase velocity to be the higher, the higher the frequency. For a given frequency, phase shift is the less, the higher the tail-end pressure p_2, the less the friction factor λ, and the larger the pipe size. The diagram denoted (g) shows the amplitude ratio to decrease with pipeline length; the diagram denoted (h) shows the phase shift to increase with it. — This way of satisfying consumer demand has for its main advantage that no pressure energy need be dissipated by throttling at the tail end, that is the power consumption of compressor is reduced. A precondition of any application of this method is, of course, a sufficiently accurate foreknowledge of the demand wave, in the form of the relevant relationships $q_1 = f'(t)$ and $p_1 = f''(t)$; also, the compressor station should be operated in keeping with these relationships.

No analytic solution of general validity is known for the system of partial differential equations discussed as describing transient gas flow in Section 8.4.1. In special cases, however, connected with specific initial and boundary conditions, the system of equation can be solved. Literature contains descriptions of many such solutions (e.g. Komikova 1971, Wilkinson et al. 1964). One of the common traits of these solutions is that they permit the analysis of partial problems and that their computer time demand is not excessive. In practice, numerical solutions are often preferred in simulating transient flow conditions.

(b) Numerical solutions

In the approach to the numerical solution of the system of partial differential equations 8.4—4 and 8.4—5, the system is transformed into a system of algebraic equations using the method of finite differences. This algebraic system is capable of solution. For the transformation, the method of central finite differences can be used to advantage. It consists in essence of replacing the function, continuous in the interval under investigation, by a chord extending across a finite domain of the independent variable. The slope of said chord is approximately equal to the slope of the tangent to the curve at the middle of the domain. It is subsequently simple to calculate numerically the derivative of the curve.

For solving the system of differential equations, literature (e.g. Zielke 1971) usually cites three methods: *the implicit method, the explicit method and the method of characteristics.* A common trait to the three methods is that calculation proceeds step by step, deriving pressures and flow rates prevailing at various points of the pipeline at the instant $t + \Delta t$ on the basis of the known distribution of pressures and flow rates at the instant t. The differences are as follows. — In the explicit method, the partial differential equations are transformed into algebraic equations, so that the unknown pressures and flow rates at the instant $t + \Delta t$ depend only on the known pressures and flow rates of the preceding time step, which permits us

to find their values one by one solving the individual equations for them. — In the implicit method, a system of algebraic equations results, which contains the unknown pressures and flow rates at the instant $t + \Delta t$ at the neighbouring points of the pipeline so as to be made available only by the solution of the entire simultaneous set of equations. The system of equations furnished by the transformation may, in both cases, be either linear or not. There is the fundamental difference that, whereas in the explicit system the time step is limited for reasons of stability, the only consideration that limits the time step in the implicit method is the accuracy required, but steps are usually significantly longer than what is admissible in the explicit

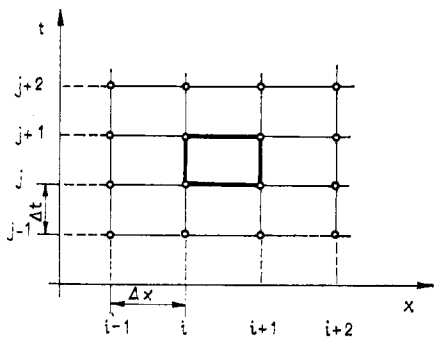

Fig. 8.4—5

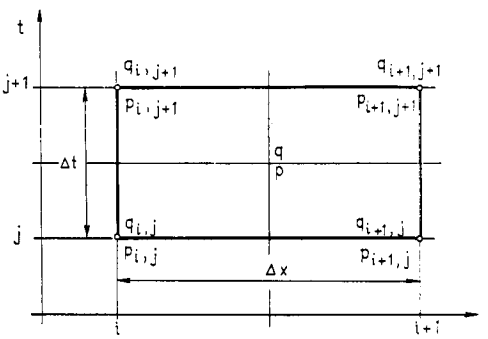

Fig. 8.4—6

method. — The method of characteristics is essentially an explicit method whose essence is to seek in the $[x, t]$ plane such directions along which the partial differential equation can be reduced to a common differential equation. This latter can be solved numerically by the method of finite differences. The time step is rather restricted also in this method.

Let us now discuss the transforming of the system of partial differential equations into one of algebraic equations by the method of finite differences as performed in the implicit method (Streeter and Wylie 1970, Zielke 1971). The pipeleg under examination is divided up into segments of length Δx. The time-variable flow rates and pressures of the line sections thus obtained can be assigned to the nodes of the lattice in Fig. 8.4—5, with a distance step Δx and a time step Δt. Figure 8.4—6 is a blow-up of the cell bounded by the lattice points $(i;\ i+1)$ in space and $(j;\ j+1)$ in time. On the basis of this Figure, approximate values for the derivatives figuring in the systems of partial differential equations 8.4—4 and 8.4—5, relative to said cell, can be written up (with q_m replaced by q) as follows:

$$\frac{\partial p^2}{\partial x} = \frac{p^2_{i+1,j+1} + p^2_{i+1,j} - p^2_{i,j+1} - p^2_{i,j}}{2\Delta x} \qquad 8.4-14$$

$$\frac{\partial p}{\partial t} = \frac{p_{i,j+1} + p_{i+1,j+1} - p_{i,j} - p_{i+1,j}}{2\Delta t} \qquad 8.4-15$$

$$\frac{\partial q}{\partial x} = \frac{q_{i+1,j+1} + q_{i+1,j} - q_{i,j+1} - q_{i,j}}{2\Delta x} \qquad 8.4-16$$

$$\frac{\partial q}{\partial t} = \frac{q_{i,j+1} + q_{i+1,j+1} - q_{i,j} - q_{i+1,j}}{2\Delta t} . \qquad 8.4-17$$

Regarding pressure p and mass flow rate q figuring in Eqs 8.4—4 and 8.4—5 as time and space averages that are constant within the cell, we get

$$q = \frac{1}{4}(q_{i,j} + q_{i+1,j} + q_{i,j+1} + q_{i+1,j+1}) \qquad 8.4-18$$

$$p = \frac{1}{4}(p_{i,j} + p_{i+1,j} + p_{i,j+1} + p_{i+1,j+1}). \qquad 8.4-19$$

Resubstituting Eqs 8.4—14—8.4—19 into Eqs 8.4—4 and 8.4—5, and rearranging, we have a system of non-linear algebraic equations:

$$\left.\begin{aligned}
F_1 &= \frac{1}{\Delta t}(p_{i,j+1} + p_{i+1,j+1} - p_{i,j} - p_{i+1,j}) + \\
&+ \frac{B^2}{A\Delta x}(q_{i+1,j+1} + q_{i+1,j} - q_{i,j+1} - q_{i,j}) = 0 ; \\
F_2 &= \frac{1}{\Delta x}(p^2_{i+1,j+1} + p^2_{i+1,j} - p^2_{i,j+1} - p^2_{i,j}) + \\
&+ \frac{1}{2A\,\Delta t}(p_{i,j} + p_{i+1,j} + p_{i,j+1} + p_{i+1,j+1}) \times \\
&\times (q_{i,j+1} + q_{i+1,j+1} - q_{i,j} - q_{i+1,j}) + \\
&+ \frac{g \sin\alpha}{4B^2}(p^2_{i,j} + p^2_{i+1,j} + p^2_{i,j+1} + p^2_{i+1,j+1}) + \\
&+ \frac{\lambda B^2}{8d\,A^2}(q_{i,j} + q_{i+1,j} + q_{i,j+1} + q_{i+1,j+1}) \times \\
&\times |q_{i,j} + q_{i+1,j} + q_{i,j+1} + q_{i+1,j+1}| = 0.
\end{aligned}\right\} \qquad 8.4-20$$

If the values of the parameters $q_{i,j}$; $q_{i+1,j}$; $p_{i,j}$; $p_{i+1,j}$ at the instant j are known, either because they figure in the initial conditions or as a result of the calculation for a preceding time step, then the pair of equations contains four unknowns in all: the parameters $q_{i,j+1}$; $q_{i+1,j+1}$; $p_{i,j+1}$; $p_{i+1,j+1}$, belonging to the instant $t + \Delta t$. The pair of equations 8.4—20 may be written up in a similar manner for each one of the n cells. Thus, in any time step, we have to solve $2n + 2$ equations, including the two boundary conditions, for $2n + 2$ unknowns altogether. For solving the

$2n + 2$ non-linear algebraic equations, Streeter and Wylie (1970) have proposed the Newton—Raphson method of iteration. The procedure of solution is influenced by the way the two boundary conditions are stated; it will differ according to whether the two boundary conditions refer to the same or to opposite ends of the pipe segment examined. Said boundary conditions are most often time functions of node gas flow rate or pressure. — The number of steps of iteration required to solve the system of equations depends to a significant extent on the choice of initial values for the variables. In order to accelerate convergence it is to be recommended to estimate the initial values by extrapolating from the values found for the preceding time steps. A solution of sufficient accuracy of the system of equations may thus be achieved in just one or two steps. The implicit method has the advantage of being stable even if the time steps Δt exceed $\Delta x/B$, and that, consequently, time-step length is limited by accuracy considerations only. There is, however, the drawback that the values of the variables for the instant $t + \Delta t$ may occasionally be furnished by a non-linear system of equations of almost-unmanageable size.

The method of characteristics has also been employed (Streeter and Wylie 1970) for the solution of Eqs 8.4—4 and 8.4—5. The advantages and disadvantages of this method resemble those of the explicit method; all there is to do in order to find the pressure and mass flow rate in the next instant of time is the solution of a system of two quadratic equations in two unknowns, but the time step, for reasons of stability, must be quite small: $\Delta t < \Delta x/B$. There is an advantage in simultaneously using the characteristic and the implicit method. This will increase the largest admissible time step Δt rather significantly against what is admitted by the sole use of the method of characteristics. Furthermore, the method of characteristics permits the breakdown of complex gas transmission systems into simpler elements. The implicit method, applied to the individual elements, will yield a smaller number of non-linear equations per system, and accordingly, time needed to solve these equations will be reduced rather substantially.

8.4.3. Flow in pipeline systems

If there is injection or offtake of gas at certain intermediate points of the transmission line, then these points are to be regarded as nodes and the node law must apply to them. The system of non-linear algebraic equations, written up for the implicit cells of the individual pipeline segments and composed of pairs of equations resembling Eqs 8.4—20, is then complemented by node continuity equations of the form

$$q_n + \sum_{i=1}^{m} q_i = 0 ,$$

where q_n is the gas mass flow into or out of the node, and the q_is are the mass flow rates in the pipelegs meeting at the node. It is the solution of this extended non-linear system of algebraic equations that furnishes the time-

dependence of pressures and flow rates in a transmission line with injections and offtakes at intermediate points. Describing in this way the transients taking place in the transmission line system is fairly complicated; this is why, despite its accuracy, it is used to solve simpler, radial systems only (Wylie et al. 1970). Modelling the transients of more complicated, looped nets is usually performed by some simpler method resulting from certain neglections. The most usual neglections are as follows (Guy 1967).

In a gas transmission line system, neglecting the altitude difference between the system's nodes does not usually introduce a significant error. The third-term on the right-hand side of Eq. 8.4—5 describing transient flow may therefore be dropped. It can further be shown that the term $(p/A_i)(\partial q/\partial t)$, describing the change per unit of time in the rate of mass flow on the right-hand side of Eq. 8.4—5, is in the majority of practical cases less by an order of magnitude than the friction term

$$\frac{\lambda B^2 q^2}{2 d_i A_i^2},$$

and is therefore negligible, too. These simplifications reduce the system composed of Eqs 8.4—4 and 8.4—5 to the following, much simpler, form:

$$\frac{\partial p}{\partial t} = -\frac{B^2 \partial q}{A \partial x}, \qquad 8.4-21$$

$$\frac{\partial p^2}{\partial x} = \frac{\lambda B^2}{\mathrm{d}A^2} q^2, \qquad 8.4-22$$

where we have changed the notation concerning internal cross-sectional area and *ID* of the pipe ($A_i \rightarrow A$; $d_i \rightarrow d$). — Equation 8.4—21 states the pressure change per unit of time in an infinitesimal length of pipe $\mathrm{d}x$, brought about by an infinitesimal change in the gas mass flow rate. The equation describes the capacitive property of the pipeline. — By Eq. 8.4—22, the flowing pressure drop in the infinitesimal length of pipe $\mathrm{d}x$ can be calculated using the relationship for steady-state flow. The equation expresses the resistance to flow of the pipeline. The physical content of these equations can be generalized to systems of pipelines as follows.

One assigns to any node half the length of each pipeleg tying in to that node, and the half-legs thus obtained are summed. Let the volume thus assigned to node j be V_j. The flows $q_{i,j}$ into and out of the node and the offtake $q_{o,j}$ at the node determine the change of the mass flow rate at the node. Equation 8.4—21 may, therefore, be rewritten for this node in the following form (Fincham 1971):

$$\frac{V_j \mathrm{d}p_j}{B^2 \mathrm{d}t} = \sum_{i=1}^{m} q_{i,j} - q_{o,j} \qquad 8.4-23$$

where m is the number of pipelegs tying in to the node. — By Eq. 8.4—22,

mass flow rates in the pipelegs assigned to node j can be calculated using the relationship

$$q_{i,j} = \left[\frac{d_{i,j} A_{i,j}^2}{\lambda_{i,j} B^2} \frac{| p_i^2 - p_j^2 |}{l_{i,j}} \right]^{0.5} S_{i,j} \qquad 8.4-24$$

where the $l_{i,j}$s are the lengths of the individual pipelegs and

$$S_{i,j} = \text{sign}\,(p_i - p_j).$$

Introducing Eq. 8.4—24 into Eq. 8.4—23, and employing the notation

$$K_j = \frac{B}{V_j} \quad \text{and} \quad J_{i,j} = J_{j,i} = \left(\frac{\mathrm{d}A^2}{\lambda l} \right)_{i,j}^{0.5}$$

we get after rearranging the differential equation

$$\frac{\mathrm{d}p_j}{\mathrm{d}t} = K_j \sum_{i=1}^{m} [J_{i,j}(| p_i^2 - p_j^2 |)^{0.5} S_{i,j}] - q_{oj}. \qquad 8.4-25$$

Applying the method of finite differences,

$$\frac{\mathrm{d}p_j}{\mathrm{d}t} = \frac{p_j(t + \Delta t) + p_j(t)}{\Delta t}.$$

Using this, Eq. 8.4—25 assumes after rearranging the form

$$p_j(t + \Delta t) = \Delta t\, K_j \Big\{ \sum_{i=1}^{m} [J_{i,j}(| p_i^2 - p_j^2 |)^{0.5} S_{i,j}] - q_{oj} \Big\} + p_j\, t\,. \qquad 8.4-26$$

Writing up similar equations for the other nodes we obtain a system of non-linear algebraic equations concerning the transients in the complex system. The solution of this system of equations furnishes the pressures prevailing at the individual nodes at the instant $(t + \Delta t)$. Differential equation 8.4—25 can be solved using the implicit or explicit method, as follows.

Let us introduce the notation

$$C_j = \Delta t\, K_j \Big\{ \sum_{i=1}^{m} J_{i,j}(| p_i^2 - p_j^2 |)^{0.5} S_{i,j} - q_{oj} \Big\}.$$

Equation 8.4—26 may accordingly be written up in two ways:

$$p_j(t + \Delta t) = C_j(t) + p_j(t)$$

for the explicit method, and

$$p_j(t + \Delta t) = C_j(t + \Delta t) + p_j(t)$$

for the implicit method. If the node pressures at the instant t are fixed by some initial condition, then the explicit method will directly furnish the pressures prevailing at the instant $(t + \Delta t)$. If, on the other hand, the implicit method is adopted, then said pressures may be obtained only by simultaneously solving the system of non-linear algebraic equations,

including an equation resembling 8.4−26 for each node. If the system incorporates other elements (compressor, choke, etc.) as well, then the models described so far are further complicated. These elements having no transient storage capacity, however, their transient behaviour will be characterized by the same mathematical models as are described in Section 8.3.1 for steady-state operation.

In connection with the application to concrete cases of the mathematical models outlined above, we have invariably pointed out the necessity of formulating suitable initial and boundary conditions. The alternatives arising in this respect were summarized by Batey et al. (1961).

In fixing initial conditions there are two options. (i) Flow rates and pressures are determined by simultaneous measurement at various points of the pipeleg examined, and the pressure and flow rate distribution functions thus obtained will fix the initial state of the system. This procedure is bound to run up against a number of difficulties, and it is therefore much more common that: (ii) flow is considered as steady-state at the instant $t = 0$ in the pipeleg examined. The initial pressure distribution required for the transient calculation can then be calculated using the steady-state model, and the mass flow rate is constant.

In defining boundary conditions, the following alternatives enter into consideration. One may fix the variation in time of the injection or delivery pressure, of the flow rate or of throughput. As these six parameters are not independent mathematically, it is necessary and sufficient to fix the time variations of two parameters. In a complex system it is usually necessary to start from time-variable consumer demand at the various nodes. The mathematical formulation of the relevant time functions may be based e.g. on the harmonic analysis of measurement results. Once the time functions have been established, one of the problems to be solved may be the adjustment, within the feasible limits, of the flow rates and pressures of the individual sources of gas, and possibly of compressor horsepower, so that the pressures at the consumer offtake points do not exceed the least supply pressure contracted for by more than a certain safety reserve. This is the way in which energy losses due to expansion can be minimized.

8.5. Computer modelling of gas transmission systems

8.5.1. Case of the digital computer

The practical mathematical modelling of gas transmission systems has been made possible by the advent of the high-speed electronic computer. This statement is amply illustrated by the computation time demand of the steady-state, let alone the transient, network models described above. Employing the digital computer for systems modelling requires the mathematical formulation, 'intelligible' to the computer, of the fundamental data (e.g. system configuration) and of the fundamental relationships describing the particular model envisaged. This formulation is something of a special

problem. In solving it, the systems analyst is assisted by an independent branch of modern mathematics, graph theory (Haray 1969), which has been applied—e.g. by Szendy (1967)—to the topological characterization of electric networks, too.

(a) Application of the graph theory

The complex gas transmission system composed of nodes and NCEs may, with due attention to the known or assumed directions of flow, be regarded as a directed graph whose connection matrix **A** is rather simple to write up. Let the columns of **A** represent NCEs, that is, edges of graph, and let the rows represent nodes. Let element a_{ij} of the matrix be

$$a_{i,j} = \begin{cases} +1, & \text{if edge } j \text{ emerges from node } i, \\ -1, & \text{if edge } j \text{ ends in node } i, \\ 0, & \text{if edge } j \text{ and node } i \text{ are unconnected.} \end{cases}$$

The connection matrix of the graph in Fig. 8.5—1a, representing the network in Fig. 8.3—6, is accordingly

$$\mathbf{A} = \begin{array}{c|cccccccccccc} & 1 & 2 & 3 & 4 & 5 & 6 & 7 & 8 & 9 & 10 & 11 & 12 \\ \hline 1 & 1 & 0 & 0 & 1 & 0 & 0 & 0 & 0 & 0 & 0 & 0 & 0 \\ 2 & -1 & 1 & 0 & 0 & 0 & 0 & 0 & 0 & 0 & 0 & 0 & 1 \\ 3 & 0 & -1 & -1 & 0 & 0 & 0 & 0 & 0 & 0 & 1 & 1 & 0 \\ 4 & 0 & 0 & 1 & -1 & 1 & 0 & 0 & 0 & 0 & 0 & 0 & 0 \\ 5 & 0 & 0 & 0 & 0 & -1 & 1 & 0 & 0 & 0 & 0 & 0 & 0 \\ 6 & 0 & 0 & 0 & 0 & 0 & -1 & 1 & 0 & 0 & 0 & -1 & 0 \\ 7 & 0 & 0 & 0 & 0 & 0 & 0 & -1 & -1 & 0 & 0 & 0 & 0 \\ 8 & 0 & 0 & 0 & 0 & 0 & 0 & 0 & 1 & -1 & -1 & 0 & 0 \\ 9 & 0 & 0 & 0 & 0 & 0 & 0 & 0 & 0 & 1 & 0 & 0 & -1 \end{array} \quad \text{Nodes} \qquad 8.5-1$$

Node-connecting elements

This connection matrix uniquely defines system configuration. In network calculation, one requires in addition to the connection matrix also a definition of the loops—the senses of rotation—in the network, which

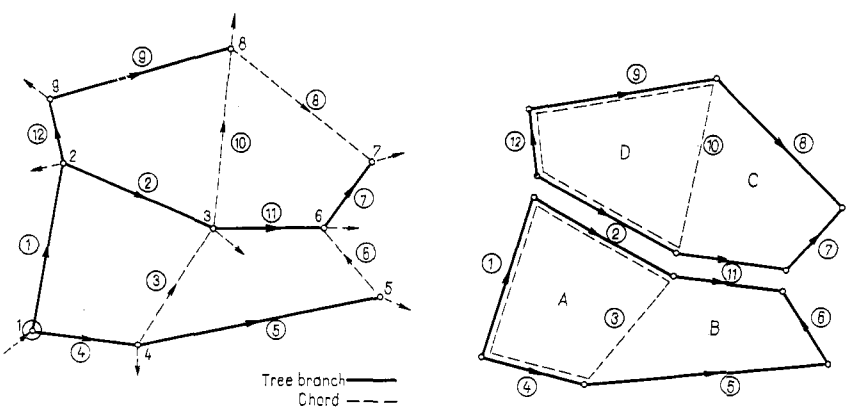

Fig. 8.5—1 Gas transmission system

may be performed with the aid of the so-called loop matrix. In order to derive the loop matrix from the connection matrix it is necessary to introduce the concept of a tree. This term denotes a connected graph in which there is one and only one trajectory between any two nodes. Thus, any loopless graph is a tree. If a graph is looped, it is possible to turn it into a tree by eliminating some of its edges. This may be performed automatically, by adding up the rows of the connection matrix. Let us designate on the tree chosen a so-called point of reference or base point, and let us drop the corresponding row from the connection matrix. Now rearranging the matrix so as to separate tree branches and chord branches (the latter are those which are to be eliminated to form the tree), we may write up the so-called matching matrix of the system. Let e.g. the reference point be node *1*, in the graph shown as Fig. 8.5—1a, and let us eliminate loops by dropping edges *3*, *6*, *8* and *10*. The matching matrix of the graph is, then, written in the form

$$\mathbf{B} = [\mathbf{B}_f \mathbf{B}_h] = \begin{array}{c} \\ 2 \\ 3 \\ 4 \\ 5 \\ 6 \\ 7 \\ 8 \\ 9 \end{array} \begin{array}{c} \begin{array}{cccccccc} 1 & 2 & 4 & 5 & 7 & 9 & 11 & 12 \end{array} \\ \left[\begin{array}{cccccccc} -1 & 1 & 0 & 0 & 0 & 0 & 0 & 1 \\ 0 & -1 & 0 & 0 & 0 & 0 & 1 & 0 \\ 0 & 0 & -1 & 1 & 0 & 0 & 0 & 0 \\ 0 & 0 & 0 & -1 & 0 & 0 & 0 & 0 \\ 0 & 0 & 0 & 0 & 1 & 0 & -1 & 0 \\ 0 & 0 & 0 & 0 & -1 & 0 & 0 & 0 \\ 0 & 0 & 0 & 0 & 0 & -1 & 0 & 0 \\ 0 & 0 & 0 & 0 & 0 & 1 & 0 & -1 \end{array}\right. \\ \underbrace{\qquad\qquad\qquad\qquad\qquad\qquad\qquad\qquad}_{\text{Tree branches}} \\ \mathbf{B}_f \end{array} \begin{array}{c} \begin{array}{cccc} 3 & 6 & 8 & 10 \end{array} \\ \left.\begin{array}{cccc} 0 & 0 & 0 & 0 \\ -1 & 0 & 0 & 1 \\ 1 & 0 & 0 & 0 \\ 0 & 1 & 0 & 0 \\ 0 & -1 & 0 & 0 \\ 0 & 0 & -1 & 0 \\ 0 & 0 & 1 & -1 \\ 0 & 0 & 0 & 0 \end{array}\right] \\ \underbrace{\qquad\qquad\qquad\qquad}_{\text{Chord branches}} \\ \mathbf{B}_h \end{array} \qquad 8.5—2$$

Clearly, in a graph of n nodes and m edges, the number of independent so-called basic loops is $k = m - n + 1$. It can be shown that the transpose $\mathbf{C}^T$ of the matrix $\mathbf{C}$ of these basic loops is defined by the relationship

$$\mathbf{C}^T = \begin{bmatrix} \mathbf{C}_f^T \\ \mathbf{C}_h^T \end{bmatrix} = \begin{bmatrix} -\mathbf{B}_f^{-1}\mathbf{B}_h \\ \mathbf{I} \end{bmatrix}, \qquad 8.5—3$$

where $\mathbf{I}$ is the unity matrix.

$\mathbf{B}_f^{-1}$ is the inverse of matrix $\mathbf{B}_f$. It can be produced either by inverting matrix $\mathbf{B}_f$, or by writing up directly as follows. The rows of $\mathbf{B}_f^{-1}$ are the tree branches; its columns are the nodes. Let element b_{fi}^{-1} of matrix $\mathbf{B}_j^{-1}$ be

$$b_{ji}^{-1} = \begin{cases} +1, & \text{if the trajectory from the base point to node } i \\ & \text{includes branch } j, \text{ with the branch directed towards} \\ & \text{the base point,} \\ -1, & \text{idem, with the branch directed towards the node,} \\ 0, & \text{if the trajectory from the base point to the node} \\ & \text{does not include branch } j. \end{cases} \qquad 8.5—4$$

For an example, the inverse of matrix $\mathbf{B}_f$ referring to the tree shown in continuous line in Fig. 8.5—1a, written up according to Eq. 8.5—4, is

$$-\mathbf{B}_f^{-1} = \begin{array}{c} \\ 1 \\ 2 \\ 4 \\ 5 \\ 7 \\ 9 \\ 11 \\ 12 \end{array} \begin{array}{c} \begin{array}{cccccccc} 2 & 3 & 4 & 5 & 6 & 7 & 8 & 9 \end{array} \\ \left[\begin{array}{cccccccc} 1 & 1 & 0 & 0 & 1 & 1 & 1 & 1 \\ 0 & 1 & 0 & 0 & 1 & 1 & 0 & 0 \\ 0 & 0 & 1 & 1 & 0 & 0 & 0 & 0 \\ 0 & 0 & 0 & 1 & 0 & 0 & 0 & 0 \\ 0 & 0 & 0 & 0 & 0 & 1 & 0 & 0 \\ 0 & 0 & 0 & 0 & 0 & 0 & 1 & 0 \\ 0 & 0 & 0 & 0 & 1 & 1 & 0 & 0 \\ 0 & 0 & 0 & 0 & 0 & 0 & 1 & 1 \end{array}\right] \end{array} \text{Tree branches}$$

Nodes

In possession of this inverse matrix, the transpose $\mathbf{C}^T$ of matrix $\mathbf{C}$ referring to the independent loops is obtained, after performing the matrix multiplication, written up in Eq. 8.5—3 in the form (cf. Fig. 8.5—1b):

$$\mathbf{C}^T = \left[\begin{array}{c} -\mathbf{B}_f^{-1}\mathbf{B}_h \\ \mathbf{I} \end{array}\right] = \begin{array}{c} \\ 1 \\ 2 \\ 4 \\ 5 \\ 7 \\ 9 \\ 11 \\ 12 \\ 3 \\ 6 \\ 8 \\ 10 \end{array} \begin{array}{c} \text{Loops} \\ \left[\begin{array}{cccc} A & B & C & D \\ -1 & -1 & 0 & 0 \\ -1 & -1 & -1 & 1 \\ 1 & 1 & 0 & 0 \\ 0 & 1 & 0 & 0 \\ 0 & 0 & -1 & 0 \\ 0 & 0 & 1 & -1 \\ 0 & -1 & -1 & 0 \\ 0 & 0 & 1 & -1 \\ 1 & 0 & 0 & 0 \\ 0 & 1 & 0 & 0 \\ 0 & 0 & 1 & 0 \\ 0 & 0 & 0 & 1 \end{array}\right] \end{array} \text{NCEs}$$

The system is uniquely defined by its connection matrix A and the loop matrix $\mathbf{C}$ derived from it. If in the following we agree to represent gas flow in the individual NCEs by m-dimensional column vector q, and the gas offtakes at the individual nodes by n-dimensional column vector q_o, then Kirchhoff's node law may be written in the form of a matrix equation

$$\mathbf{A}q = q_o,$$

or, in more detail, of the relationship

$$\sum_j a_{ij} q_j = q_{oi} \,.$$

Kirchhoff's second law may be written up in a similar fashion, by representing pressure changes $\Delta p^2 = p_1^2 - p_2^2$ across NCEs by column vectors ΔP. The loop law then assumes the form

$$\mathbf{C}\Delta P = 0,$$

or, in more detail,

$$\sum_j c_{kj} \Delta P_j = 0,$$

where k is the subscript of loops.

It emerges from the above considerations that modelling gas transmission systems by means of directed graphs is fairly simple; description using matrices of such systems affords a clear insight into the essence of the problem; and the calculation is readily performed by computer. It should be noted, however, that if the system is extensive, the procedure takes a considerable storage capacity. Another problem is that matrices **A**, **B** and **C** are usually highly sparse; that is, a high percentage (up to 90 or even 98 percent in some cases) of their elements may be zero. In order to reduce storage capacity demand and to simplify calculation, special sparse-matrix solution methods have been devised.

(b) Review of system-modelling programs

As a consequence of the fast-increasing popularity of the digital computer, numerous systems, simulation programs have been developed by the research teams involved with the problem. The most widely known programs were reviewed by Goacher (1969), who divided them in three main groups.

(i) General programs suitable also for the modelling of gas transmission systems. These are essentially programs suited for the solution of differential equations of various types. Several of these are included in the software of almost every medium and big general-purpose computer. The best-known such programs include CSMP (Continuous System Modelling Program (IBM 1130/360)); Digital Simulation Language (IBM 1130/7090/360); MIMIC; MIDAS (Modified Integration Digital Analog Simulation); KALDAS (Kidsrove Algol Digital Analog Simulation (ICL 1900 Series)); SLANG (Simulation Language (ICL 503/803/4120/4130/ATLAS)). These programs have the common drawback that the system of differential equations describing the process taking place in the system has to be formulated by the gas engineer, who must, in addition, bring the system to the most suitable form or, indeed, reduce it to the most fundamental operations (addition, subtraction), as the system of equations is fed to the computer as a basic data. Preparing the equations of the boundary conditions is not less cumbersome. Another disadvantage is that all programs named above employ the explicit method to solve the system of differential equations, and although the results for any time step are obtained rather fast, time steps must be quite short, which is a considerable disadvantage when handling transients of long duration.

(ii) Programs modelling steady states. These programs are used for two distinct purposes: first, independently, to investigate one of the fairly large class of steady-state or nearly-steady-state technical and engineering problems, and secondly, to furnish initial conditions for the dynamic models. The programs developed by workers of the Gas Council's London Research Station and their main characteristics are given in Table 8.5—1 (after Goacher 1969). These programs satisfy in their majority the requirement that the user should not have to know about the structure and operation of the program. The input data including the network configuration, the parameters of the pipelegs, the pressures and yields of the sources.

Table 8.5—1

Main features of steady-state network analysis programs (after Goacher 1969)

Program	Pipelegs	Nodes	Pressure-defined nodes	Loops	Compressors/Regulators
1	2	3	4	5	6
MANNA (8K)	150	150	12	15	None
MANNA (32K)	300	300	40	50	None
			50 altogether		
MANN 1 (32K)	600	500	100	200	None
			200 altogether		
SONIC (8K)	150	150	20	20	10
				20 altogether	
SONIC (32K)	300	300	40	50	20 (at least 1)
				50 altogether	
DEVIL (32K)	300	300	40	50	20 (at least 1)
				50 altogether	
SNAC (32K)	400	300	25	150	25

MANNA = Matrix Algebra for Non-linear Network Analysis (IBM 1130)
SONIC = Steady-state of Networks Including Compressors (IBM 1130)
SNAC = Steady-state Network Analysis with Compressors

and consumer demands is readily compiled with reference to a set of instructions. In order to solve a loop it is sufficient to estimate the throughput in one pipeleg included in the loop. From these data, the computer will calculate the steady-state conditions by an iteration procedure.

(iii) Programs modelling steady and transient states. In these programs, the part modelling the steady state serves to provide the initial conditions required for the transient calculations. The program is formulated also in this case so that the gas engineer in control of the system may use it as a 'black box' provided he observes certain instructions and rules of operation. Although the input data list differs from one program to the next, each program will require as a matter of course the data mentioned in connection with the programs simulating steady states. These must be complemented with the transient boundary conditions and with the parameters of the compressors, regulators, valves, etc. included in the system. The most widely known programs and their main characteristics are listed in Table 8.5—2. Not mentioned in the Table is General Electric's (USA) fairly successful GE Simulator. This latter, similarly to ENSMP and CAP, solves the differential equations by the implicit method, whereas PIPETRAN and SATAN use the explicit method. The time step is, therefore, much shorter in the latter. For an example as to the structure of a program simulating a complex gas transmission system, let us consider that of SATAN.

Table 8.5—2

A summary of the main features available in four dynamic analysis programs (after Goacher 1969)

Program	Pipelegs	Nodes	Flow-defined nodes	Pressure defined nodes	Compressors	Regulators	Loops	Valves	Flow pressure profiles	Lonble or parallel pipes
1	2	3	4	5	6	7	8	9	10	11
CAP	150	150 may have upper and lower pressure limits	No limit	5	Not available	Not available	10	10	No limit	150
ENSMP	300	300	No limit	30	20 PCO 30 altogether	Not available	10 Does not include compressor loops	Not available	5 standard type. No limit on specific type	300
PIPETRAN	105	106	30	5	10 PCO PCI FCO FCI HPC HPM	10 PCO PCI FCO FCI 50 altogether	No limit	Not available	30	105
SATAN	300	300 may have upper and lower pressure limits	No limit	25	PCO FCO HPM	PCO FCO	150	No limit	50	Not available

PCO = Pressure-controlled outlet
PCI = Pressure-controlled inlet
FCO = Flow-controlled outlet
FCI = Flow-controlled inlet
HPC = Horsepower control
HPM = Horsepower maximum
ENSMP = Extended Network Systems Modelling Program; Engineering Research Station of Gas Council (England)
CAP = Control Advisory Program; Engineering Research Station of Gas Council (England)
PIPETRAN = Pipeline Transients, Electronic Associates Inc. (USA)
SATAN = Steady and Transient Analysis of Network Gas Council London Research Station

The program consists of three main units, which may be run separately if so desired. — *Phase 1.* Calculation of the steady state. Quite often, it is necessary to compare only the steady-state operation of various system configurations, or to furnish initial conditions for the transient calculation. In that case, running this program separately, one may examine up to 10 variants in succession. At the end of each run, in addition to the printout of the desired results, all data required for the transient calculation except the boundary conditions is stored in the background memory from where

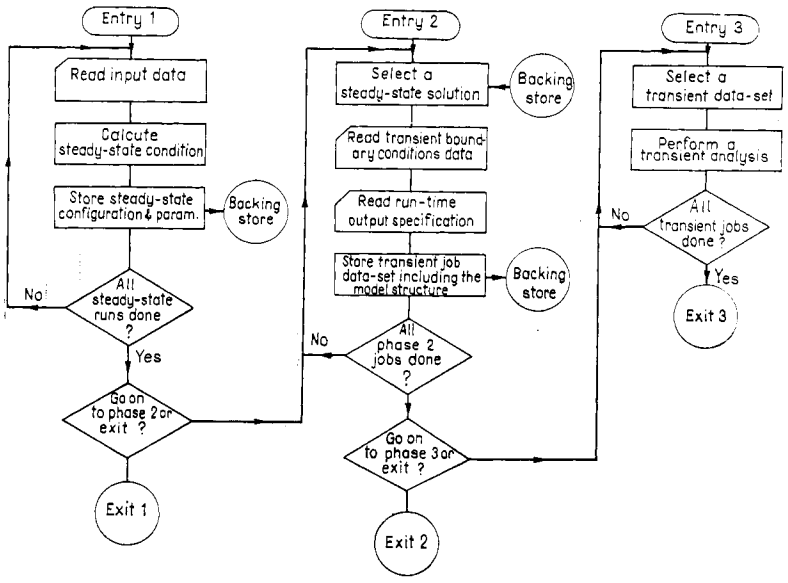

Fig. 8.5—2 The SATAN program, after Goacher (1969)

it may be called in as and when required. — *Phase 2.* This is the connecting phase in which the transient model is built up step by step out of the results of one or more variants of the previous phase, judged to be the most interesting, and out of the boundary conditions fed into the machine. The results are once more relegated to the background memory. Up to ten dynamic-model variants may be stored also in this case. — *Phase 3.* Transient analysis. The computer calls in the intermediate results, calculated in the foregoing phases, of one or several preferred variants, and calculates the transient flow rates and pressures.

The block diagram of the program is given after Goacher in Fig. 8.5—2. The program structure is such that routines providing higher accuracy, or a faster solution, or a more economical use of storage space can be introduced into the program without changing its structure, merely by exchanging certain segments.

8.5.2. Case of the analog computer

Analog computers incorporate cells simulating the four main types of elements of the gas transmission network: pipelegs, consumers, gas sources and compressor stations. The system's model can be composed of these cells by simple plug-in. In analog computers simulating steady-state flow, the so-called pipeleg cells simulating flow in a length of pipe represent the relationship

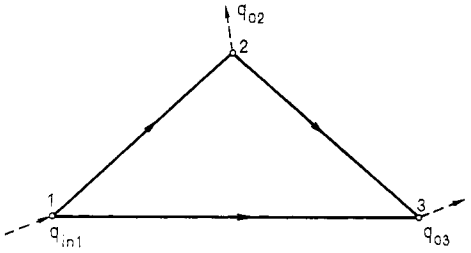

Fig. 8.5—3

$$E_1 - E_2 = RI^n$$

analogous to the friction equation, where E is E.M.F., R is electric resistance and I is intensity of current. If the variation with pressure of the flowing medium's gravity can be neglected, then pressure p in the pipeline is proportional to E. This analogy applies to low-pressure community utilities. In high-pressure gas transmission systems, where gravity varies markedly with pressure, this latter is proportional to the square root of E. The extraction of the radical is performed by a function generator. In modern apparatuses, *pipe cells* are constructed so that, if the direction of flow in a given pipeleg is opposite to what has been assumed, an automatic reversal of flow takes place. The cell simulating the consumer is a current sink which, irrespective of any voltage fluctuation at the node, absorbs current at a constant rate out of the system. The so-called *source cell* modelling the injection of gas is a d.c. power supply unit of variable output voltage. The *compressor-station cell* is an electronic amplifier.

Determining the various constants is facilitated by auxiliary diagrams in which said constants are plotted v. certain characteristic parameters, for instance, resistance to flow of a pipeleg v. pipe size and length, etc. Setting these constants by means of calibrated potentiometers is fairly simple and quick.

The results of the modelling procedure appear at a central control console, where any node or cell of the system may be called in by pushing a single button. This makes node pressure and throughput, or, in the case of a cell, the difference between input and output pressure and the gas flow rate, appear on the readouts of digital voltmeters or as a printout of a printer hooked up to the system; each data is provided with a code permitting identification. The system can be instructed to scan all nodes in succession and to record results as the scan proceeds.

In an analog system, variants of the gas-transmission-system model take much less time to build than when using a digital computer. This is a substantial advantage both when designing new systems and when examining the operation of existing ones. The analog machine can be used

to advantage also in the examination of transient behaviour. For an example let us consider one of the possible analog models of transient flow in the network section shown as Fig. 8.5—3. The principle of the procedure was outlined by Goacher (1969). The mathematical model of the network section, the system of first-degree differential equations 8.4—25, can be written in the form

$$\left.\begin{aligned}
\frac{dp_1}{dt} &= K_1\,[-J_{2,1}(p_1^2 - p_2^2)^{0.5} - J_{3,1}(p_1^2 - p_3^2)^{0.5} + q_{in1}] \\
\frac{dp_2}{dt} &= K_2\,[J_{1,2}(p_1^2 - p_2^2)^{0.5} - J_{3,2}(p) - p_3^2)^{0.5} - q_{02}] \\
\frac{dp_3}{dt} &= K_3\,[J_{1,3}(p_1 - p_3)^{0.5} + J_{2,3}(p_2 - p_3)^{0.5} - q_{03}]
\end{aligned}\right\} \qquad 8.5-5$$

The block diagram of the analog system solving this system of equations is shown as Fig. 8.5—4.

The analog computer has the considerable advantage that it will solve a variety of problems without need for mathematical abstraction, by simple manual intervention, and practically at once, with no time required for the calculation. This type of modelling is therefore of considerable interest when the problem to solve is the choice among a large number of variants in designing a new system or in optimizing an existing one. One of the applications it is best suited for is the training of transmission system operations engineers, as it lends itself very well to illustrating the way the gas supply system will function under various conditions (cf.

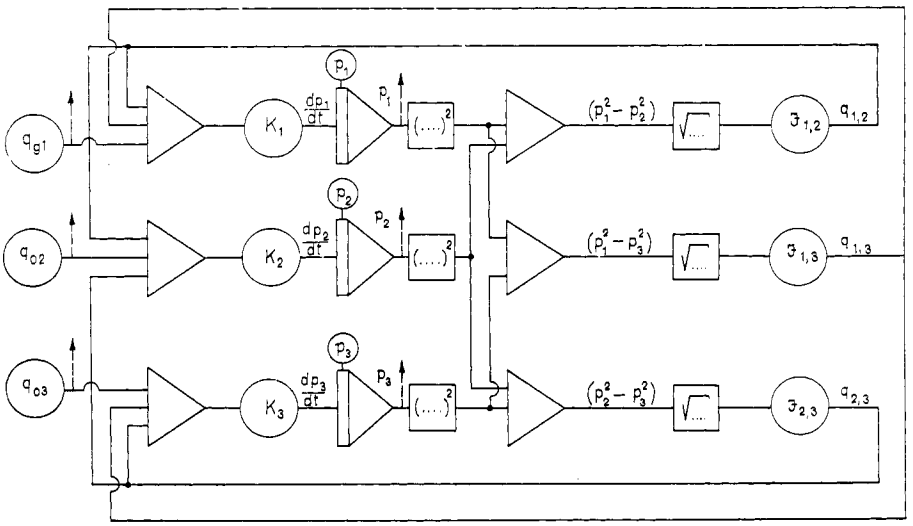

Fig. 8.5—4 Block diagram of analog setup solving the system of Equation 8.5—5, after Goacher (1969)

also Shephard and Williams 1965, de Brem and Tonnelier 1970). — The main drawback of the analog computer is that it is a special-purpose machine; a device designed for the simulation of gas supply systems, that can be used for hardly anything else. Machines suitable for representing complicated systems include a large number of cells and their price is accordingly high.

The largest-size analog computer suitable for modelling a regional gas supply system is operated by SNAM at Metanopoli, for simulating the Italian grid. After a publication in 1970, the total length of pipelines in the grid is 4000 km, and this is to be expanded by a further 5000 km. In 1968 it conveyed 10×10^9 m^3 of gas per year, and this value is expected to increase to 18 or 20×10^9 m^3 by 1980. The analog machine models 210 pipelegs, 22 injection and 70 offtake nodes, 4 compressor stations, 20 pressure regulators and 40 valves. The transient behaviour of the grid is checked every three hours. The purpose of the check is to find the most economical way of satisfying demand, in terms of minimum compressor power and optimum storage-capacity exploitation. In 1969, a digital machine was installed alongside the analog machine built in 1968. The digital machine serves to acquire measurement and situation data, to perform side calculations, to give alarm in the case of malfunctions, and to prepare reports (Bonfiglioli and Croce 1970).

8.6. Pipeline transportation of natural gas; economics

Finding the economically optimum dimensions and operating parameters of a gas transmission pipeline is a comparatively simple task if there is a single line to convey gas from the site of production to the site of consumption. If no intermediate boosting is required, then the optimum trace and pipe size of the line can be determined similarly to the method outlined for oil pipelines in Section 7.1.4. Moreover, Renauldon's procedure will furnish the most economical pipe size relatively simply even if booster stations are installed at one or more points along the pipeline (Société . . . Manuel 1968).

In practice, however, the typical problem arising is the economic optimization of transmission networks or, even more generally, of regional gas supply grids, and this is a very complicated problem indeed. As was shown in the previous section, the grid includes the gas field proper as one of its components. It was tacitly assumed that the gas flow rate out of the field is given or known. In reality, the gas reserve of the field, the envisaged rhythm of its exploitation, and its expected life will all affect economy. Measures taken in order to smooth daily and monthly production rates over the year also carry a considerable importance. We shall consider these viewpoints below.

The duration of developing a gas field (drilling the gas wells, choosing the number of producing wells, the preparation and transmission equipment to be matched to them, the capacities and the construction and installation periods of these sets of equipment) may vary rather widely.

Mayer-Gürr illustrates the economic importance of these factors on a simple example (Mayer-Gürr 1971). Figure 8.6—1a shows the first two sections of the typical production curve of a gas field, in three variants. The exploitable gas reserve of the field was assumed to equal 55 km³. Three rhythms of exploitation have been envisaged. The first production period takes five years in all three. It is during this period that production is run up to full rated capacity. This latter is 4.5 km³ in the first case, 3.0 in the second, and 2.25 in the third. This is the output that is desired to maintain over about 60 percent of the field's life. The period of level production is 10 years in the first case, 15 in the second and 20 in the third. Part (b) of the Figure shows the drilling rates and numbers of wells required by the individual variants. The reason for drilling more wells even after the run-up period of five years is that, by the assumptions made, reservoir pressure and hence the productivity of the wells will decline during production. Part (c) of the Figure shows the first cost of wells and of production equipment in the field. First cost is seen to be exactly twice as high in the first case as in the third. The rhythm of development and the prescribed sustained level of production of the gas field does, then, substantially affect the economics of the regional gas supply grid.

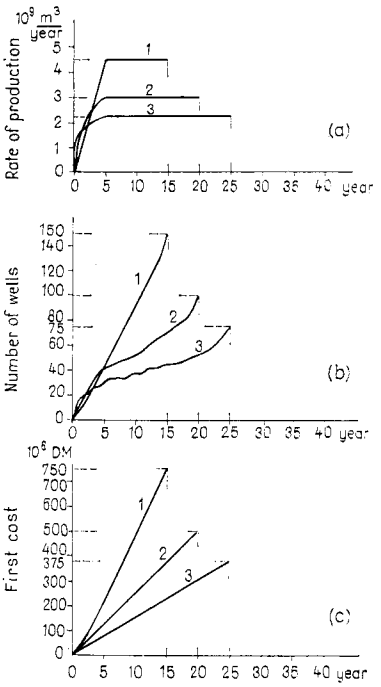

Fig. 8.6—1 Development costs of gas field, after Mayer-Gürr (1971)

The factors affecting the optimal operation of a gas supply system are, according to Graf (1971), as follows. (i) The load factor of the system should be as high as possible. (Load factor: ratio of mean to maximum hourly gas flow.) The load factor of the production system may differ from that of the supply system; the main reason for this is that one pipeline may convey gas coming from several gas fields. The gas supply company may, with a view to increasing the load factor, take the following measures: use the pipeline as a buffer storage facility (cf. Section 8.4—2a); establish an underground stratigraphic storage capacity (storage field); use a reserve of liquefied gas, or propane injection, or high-pressure gas storage to ensure an excess supply capacity for periods of peak demand. (ii) Of the above-enumerated measures, those are taken that ensure the most economical solution in any given case. (iii) Gas fields of various nature are to be produced in the most economical combination, possibly one after another. (iv) The system should ensure uninterrupted gas supply with a high degree of safety. The safety of supply can be measured by two factors.

One is availability, which is the ratio of the aggregate length of uninterrupted supply periods to total time. The other is the reserve factor. The higher the availability the less reserve is needed in the form of parallel lines, underground storage capacity or standby peak-demand supply systems.

Undergound storage in storage fields is a chapter of reservoir engineering. Here we shall just touch upon the essentials and the nature of the procedure. Natural gas may be stored in a gas reservoir, either exhausted or nearing exhaustion, in an exhausted crude oil reservoir, or in an aquifer. Requirements facing a reservoir are as follows. (i) It should have a cap-rock impervious to gas, (ii) it should have sufficiently high porosity and permeability, (iii) the storage wells should not establish communication betwen the formations traversed, that is, their casings should be cemented in so as to provide faultless packoff (isolation); (iv) it should be situated close to the area of consumption, (v) the reservoir rock should be chemically inert vis-à-vis the gas to be stored. — The gas reservoir may be closed, with no inflow of water from below or laterally. The storage space may in such cases be regarded in a fair approximation as a closed tank whose volume equals the pore volume. In open reservoirs, decrease of pressure entails the inflow of water from below or from the periphery towards the centre of the reservoir. On the injection of gas into the reservoir, the gas–water interface will sink. The gas-filled volume of this type of underground reservoir is, then, variable. In the USA, underground storage reservoirs for the storage of natural gas have been in use since 1915, and G. C. Grow (1965) predicted the volume of such reservoirs to attain 35 percent of country-wide annual consumption by 1980.

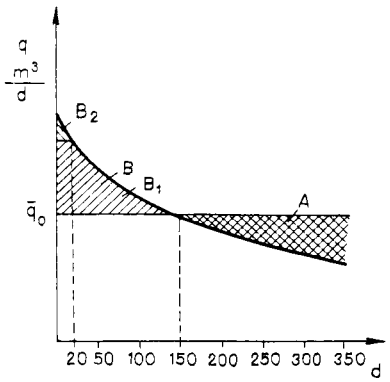

Fig. 8.6—2 Natural gas supply (after Kridner 1965)

The main purpose of an underground storage reservoir is to mitigate the economically harmful influence of seasonal fluctuations in demand. Such fluctuations are significant especially where one of the foremost uses of gas is in heating. In order to exploit the capacities of the production and transmission equipment more fully, a reserve is built up during the low-demand summer months in underground reservoirs (storage fields) close to consumption centres. This is where peak demand in the winter months is met from.

Figure 8.6—2 is a typical diagram of natural-gas supply. The bold line shows the number of days on which daily consumption exceeds some arbitrary daily consumption q_i. The area below the curve equals the annual gas consumption, provided the axes are suitably calibrated. The average height of the area below the curve equals the mean daily consumption, $\bar{q}$. Assuming that the production equipment produces, and the transmission

system conveys, a gas flow q each day, the area A indicates the volume of gas that can be stored up in the low-demand period. Area B, equal to area A, is proportional to the volume of gas to be taken out of the reservoir on high-demand days. The diagram reveals that, in the case considered, gas will have to be taken out of the reservoir over 150 days. Area B is split in two parts. Gas volume B_1 is most expediently stored in a storage field, whereas the storage of volume B_2 by some other means may be more economical, because taking out B_2 of the storage field would need a fairly

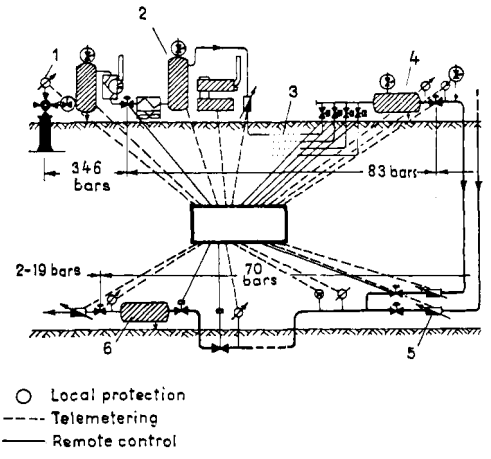

Fig. 8.6—3 The German Federal Republic's gas supply system, after Graf (1971)

considerable increase of the gas production capability of the producing field, which is rather a costly affair. It may therefore be expedient to supply volume B_2 from, for example, high-pressure undergound gas tanks, storage of liquefied gas, or of propane gas, etc. These methods have a copious literature.

Regional gas supply grids are usually too complicated to be operated optimally by unassisted men, in view of the continually changing demand and other conditions facing the system. This is why the process control of such systems is of so great an importance. Today's consensus is that joint off-line control by man and computer is to be preferred. One of the tasks of the computer is data acquisition and the presentation in due time of adequate information. In possession of this information, the dispatcher must be in a position to take optimal decisions and to implement them by remote control. The other main task of the computer is the on-line control of certain functions (Holland and Mix 1970). The first publication on off-line process control dates from 1966 (*Pipe Line News* 1966). Process control of gas supply systems has considerably spread since. Roberts (1970) describes the gas supply grid of Panhandle Eastern, controlled by a dispatcher assisted by an IBM-1800 computer. The grid incorporates

pipelines of 2100 km aggregate length and supplies with natural gas 110 utilities catering to 22 million consumers. — Let us cast a brief glance on computer control, with the system realized at the Brigitta-Mobil Oil companies taken as an example. Figure 8.6—3 is a schematic sketch of the journey of natural gas from the gas wells to the consumers. Gas is produced from wells *1*, and led through the dehydrators *2* installed next to each well into flowline *3* and through it into well centres *4*. From there, gas flows through transmission line *5* and enters the low-pressure utility

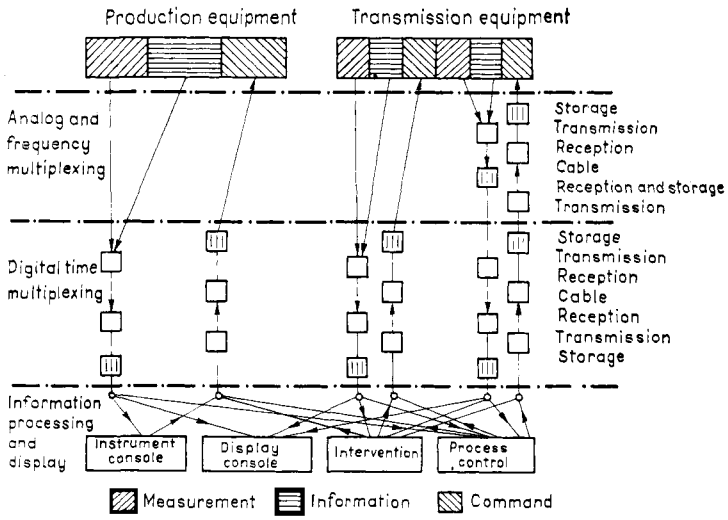

Fig. 8.6—4 Information transfer, display and control (Mittendorf and Schlemm 1971)

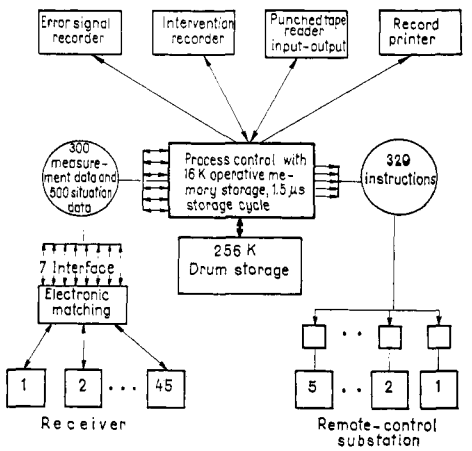

Fig. 8.6—5 Flow of information among telemetering, remote-control and program-control equipment (Mittendorf and Schlemm 1971)

at transfer station *6*. The data acquired all over the system is supplied to the central process control at Visbek. Critical points are provided with local automatic safety equipment (Graf 1971).

Figure 8.6—4 is a schematic diagram of information flow and control (Mittendorf and Schlemm 1971). It is seen that both the dispatcher and the computer may give commands controlling both the production and transmission equipment. — Figure 8.6—5 shows information flow between the computer, its peripheral units, and the remote-signalling and remote-control equipment.